ASPECT
FACILITATING SEAMLESS CLIMATE ADAPTATION

D3.3 A representation catalogue of extreme events in convective permitting resolution

June 2026

Yi-Chi Wang (SMHI)

Aitor Aldama Campino (SMHI)

Fuxing Wang (SMHI)

Danijel Belušić (University of Zagreb)

Petter Lind (SMHI)

Ralf Döscher (SMHI)

Funded by the European Union

This project has received funding from the European Union's Horizon Europe research and innovation programme under grant agreement Nº 101081460.

Document information

D3.3 A representation catalogue of extreme events in convective permitting resolution	
Grant Agreement number	101081460
Project title	Adaptation-oriented Seamless Predictions of European ClimaTe
Project acronym	ASPECT
Project start date	1 January 2023
Project duration	48 months
Work Package	WP3
Deliverable lead	Swedish Meteorological and Hydrological Institute (SMHI)
Author(s)	Yi-Chi Wang (SMHI) Aitor Aldama Campino (SMHI) Fuxing Wang (SMHI) Danijel Belušić (University of Zagreb) Petter Lind (SMHI) Ralf Döscher (SMHI)

Type of deliverable* (R, DEM, DEC, other)	R
Dissemination level** (PU, CO, CI)	PU
Date of first submission	30 June 2026
Revision n°	-
Revision date	-

Please cite this report as: Wang, Y., Aldama Campino, A., Wang, F., Belušić, D., Lind, P., Döscher, R. (2026), A representation catalogue of extreme events in CP resolution, D3.3 of the ASPECT project.

Disclaimer: *Funded by the European Union. Views and opinions expressed are, however, those of the author(s) only and do not necessarily reflect those of the European Union or the European Climate, Infrastructure and Environment Executive Agency (CINEA). Neither the European Union nor the granting authority can be held responsible for them.*

*** R**=Document, report; **DEM**=Demonstrator, pilot, prototype; **DEC**=website, patent fillings, videos, etc.; **OTHER**=other

**** PU**=Public, **CO**=Confidential, only for members of the consortium (including the Commission Services), **CI**=Classified

Table of Contents

Executive Summary 6
About ASPECT 8
1 Introduction & scientific rationale 8
1.1 Project context 8
1.2 Introduction of Emilia-Romagna region and extreme event characteristics 10
2. Methodology and data: 12
2.1 Data used for validation 12
2.1.1 Reference local data: ERG5 13
2.1.2 E-OBS 14
2.1.3 ESA Climate Change Initiative soil moisture climate data 14
2.1.4 ERA5 reanalysis 14
2.2 The EBD pipeline 15
2.2.1 Event detection strategy: 17
2.2.1.1 Threshold-based method 17
2.2.1.2 Circulation-based method 18
2.2.2 Modeling framework 18
2.2.2.1 HCLIM and domain setup: 18
2.2.2.2 Initialization : soil spin-up procedure 20
2.2.2.3 Initialization : sensitivity to atmospheric spin-up initial dates 20
2.2.3 Event-specific development 22
2.2.3.1 Heatwave specialization: soil moisture restoration practice 22
2.2.3.2 Extreme rainfall specialization: ensemble boosting 25
2.3 30-year prediction framework with SMHI-LENS 26
2.4 Extreme event analysis 28
3. Description of the event catalogue 29
3.1 Catalogue architecture 29
3.2 Event selection criteria 30
3.3 Data format and variables 31
4. Evaluation & performance 32
4.1 Extreme rainfall analysis: 32
4.1.1 Validation of rainfall spectrum in SMHI-LENS Recent Climate and ERG5 32
4.1.2 Validation of intensity statistics in EBD-SMHI-LENS Recent Climate 33
4.1.3 Validation with large-scale circulation related to EPE in Recent Climate 35
4.2 Heatwave analysis : 36
4.2.1 Validation of Tmax statistics in SMHI-LENS in Recent Climate 36

4.2.2 Validation of heatwave events in EBD-SMHI-LENS in Recent Climate 38
5. Uncertainty & methodology constraints 40
5.1 GCM and scenario dependency 41
5.2 Detection sensitivity 41
5.3 Initialization Risks 44
6. Synthesis: future climate signals 45
6.1 Rainfall dynamics 45
6.2 Heatwave Dynamics 49
6.3 Synthesis: 53
7. Future applicability of scalable prototype 55
References 57
Supplementary Material 61

Executive Summary

This deliverable presents the development and application of the Event-Based Downscaling (EBD) framework within the ASPECT project to generate actionable climate information for high-impact climate extremes in the Emilia–Romagna region of northern Italy. Developed in close collaboration with the regional stakeholder ARPAE, the framework addresses two priority climate hazards identified through the co-design process: extreme precipitation associated with regional flooding and prolonged urban heatwaves.

The work demonstrates the flexibility of the EBD approach to investigate different types of climate extremes within a common methodological framework. By combining large climate-model ensembles, targeted event selection, and high-resolution dynamical downscaling, the framework generates physically consistent ensembles of extreme-event realizations and provides event-focused climate information beyond conventional climate projections. The resulting event catalogue enables the assessment of event characteristics, probability distributions, and return levels that are directly relevant for climate-risk assessment and adaptation planning in Emilia–Romagna.

The deliverable contributes directly to the objectives of WP3 by demonstrating a prototype climate-service workflow for stakeholder-oriented climate information. For extreme precipitation, the EBD framework successfully reproduces the large-scale circulation and moisture-transport patterns associated with heavy-rainfall events over northern Italy, while highlighting the added value of convection-permitting simulations for representing localized and convective precipitation extremes. The results suggest a tendency toward increased moderate-to-strong rainfall events (return periods below approximately 10 years) under warmer mid-century climate conditions, whereas the most extreme events show a tendency toward reduced occurrence. However, the robustness of this signal remains uncertain because of limited event samples, sensitivity to event-detection methods, and the substantial uncertainties associated with estimating rare events.

A central outcome of this work is the demonstration that EBD can provide physically plausible, stakeholder-relevant climate information while explicitly accounting for uncertainty. The analyses highlight the importance of uncertainties arising from event-detection methodologies, event sampling, and statistical estimation procedures,

particularly for rare high-impact events. As a prototype application, the study further illustrates the need to consider additional sources of uncertainty associated with the choice of climate model, warming storyline, and regional downscaling configuration when interpreting future climate risks.

About ASPECT

ASPECT aims to establish and demonstrate seamless climate information (SCI) systems with a time horizon of up to 30 years, supported by underpinning research and tailored climate information for sectoral applications. The project improves existing climate prediction systems and merge outputs with projections across timescales into a harmonized SCI framework for decision-making. A key component is the provision of regional climate information through advanced downscaling approaches including statistical methods, analogs and high-resolution convection-permitting dynamic models to better represent extremes and local impacts.

The project focuses on European climate information while also addressing regions of wider European policy interest, such as disaster preparedness. ASPECT maintains strong links with WCRP lighthouse activities to advance understanding and prediction of Earth system change. To provide a broad and robust range of information, the SCI system relies on multi-model climate forecasts and builds on experiences from projects such as EUCP, while aligning with European Digital Twin initiatives including DestinE. The SCI integrates physical climate science with insights from other disciplines to ensure relevance, reliability, and usability for user-driven decision contexts. The information package includes baseline forecasts and projections with uncertainty estimates and explores new frontiers such as high-impact extremes.

Research activities address understanding and attribution of processes across timescales, including signal-to-noise issues and predictability, improved system initialization, merging predictions with projections, and innovative post-processing methods to enhance forecast skill and robustness. Particular emphasis is placed on regionalization and downscaling strategies that translate large-scale climate information into actionable local-scale products for impact- and event-focused applications.

1 Introduction & scientific rationale

1.1 Project context

The deliverable D3.3 is addressing the following WP3 objective:

- Deliver new, actionable climate data to support climate adaptation efforts, featuring high spatial resolution and temporally seamless presentation.

The expected results are categorised into methodologies and products for spatial downscaling (task 3.2) and temporal merging (task 3.3). To ensure that the outputs are demand-driven, WP3 establishes strong connections between scientific developments and the climate information needs of decision-makers, with a particular focus on ASPECT use cases; in the case of this deliverable: the governance use case.

Climate downscaling is the process of providing high-resolution climate information at a regional or local scale, derived from the outputs of global climate prediction or projection models. Global climate models, whether for short-term predictions or long-term climate projections, have limitations in representing regional or local climate features due to their coarse spatial resolution. Therefore, downscaling is employed not only to enhance the spatial resolution of climate information but also to improve its physical accuracy, enhancing the relevance for specific geographic regions. While statistical downscaling methods fill an important role in e.g. relating local conditions to large scale circulation, dynamic downscaling by Convection-permitting regional climate models (CPMs) in km resolution provides additional benefits by delivering climate information at high resolution for local geographical areas which builds on physical principles.

CPMs better resolve deep convection at km-scale resolution, avoiding the need for parameterized thunderstorms used in coarser regional climate models. This leads to a much more realistic representation of intense precipitation, local extremes, and short-duration events such as flash floods and heatwaves. CPMs also improve the simulation of topographic effects, urban processes, and land–atmosphere interactions. As a result, they provide more reliable local-scale climate information for adaptation and risk assessment.

CPMs in km resolution are generally suffering from an efficiency gap by being computationally expensive. The solution provided by ASPECT is a new way of utilizing CPMs for short events only. Event-based-downscaling (EBD) consists of a process chain starting with defining a type of event, detecting those in projection of prediction models, a proper spinup and the actual simulation of the regional event in km resolution. The procedure was automatized and thus can run for literally hundreds of events, which allows for statistical analysis.

The EBD prototype developed in this project demonstrates how regional downscaling can enhance the interpretation of climate projections and predictions, particularly for extreme events that are insufficiently resolved in global models. EBD is transferable across CMIP6/CMIP7 Earth System Models providing suitable boundary conditions (originally for support of CORDEX downscaling activities). For initialized climate predictions, limited export of suitable model-level data would offer an opportunity to strengthen the integration of prediction systems with EBD. Emerging “shadowing” and “constraining” methods, connecting short-term predictions with long-term CMIP projections for seamless climate information, can provide boundary conditions for EBD beyond decadal scales. See also section 7 for more information.

In the deliverable D3.3 we provide data sets for hundreds of simulated extreme events (heat waves and precipitation) for present and future climate. This document describes the underlying concept of event-based downscaling and its prototype application in the Emilia-Romagna region.

The actual deliverable D3.3 is a data set uploaded to the project ftp server “A representation catalogue of extreme events in CP resolution” [https://aux.ecmwf.int/ecpds/home/aspect/D3.3/].

1.2 Introduction of Emilia-Romagna region and extreme event characteristics

The Emilia–Romagna region (Figure 1), located in northern Italy between the Po Valley and the northern Apennines, is characterized by strong climatic and topographic contrasts. Elevation increases rapidly from the low-lying Adriatic coastal plains in the east toward the complex mountainous terrain of the Apennines in the southwest. This pronounced transition from flat lowlands to steep orography strongly influences regional atmospheric circulation, precipitation patterns, and temperature variability (Pavan et al. 2008, Antolini et al. 2016).

Extreme precipitation events (EPEs) represent one of the most important climate-related hazards affecting Emilia-Romagna and northern Italy. The region is considered one of the European hotspots for high-intensity precipitation events because of the interaction between Mediterranean moisture transport, large-scale atmospheric circulation, and complex terrain (Grazzini et al., 2020; Cavalleri et al., 2026). Recent analyses based on convection-permitting reanalyses further indicate that northern Italy experiences some of the most intense short-duration precipitation extremes, highlighting the importance of high-resolution approaches for representing these events (Cavalleri et al., 2026). EPEs have repeatedly caused severe socio-economic damages and flooding across northern Italy. Large-scale atmospheric dynamics play a critical role in triggering these EPEs. Many severe precipitation events over northern Italy are associated with amplified upper-level Rossby wave packets and meridionally elongated troughs over western Europe (Grazzini et al. 2020, 2021). These circulation patterns promote strong meridional moisture transport toward northern Italy and the Mediterranean basin, creating favorable conditions for persistent heavy rainfall. Composite analyses further demonstrate that the most intense EPEs are linked to strong integrated water vapor transport directed toward the major orographic barriers of northern Italy, particularly the Alps and Apennines. The interaction between synoptic-scale forcing and complex topography substantially enhances flood risk across Emilia-Romagna.

The seasonal distribution of EPEs further highlights the importance of Mediterranean and topographic influences (Pavan et al. 2008, Antolini et al. 2016). EPEs occur most frequently during autumn, when the Mediterranean Sea remains warm and provides abundant atmospheric moisture. Autumn EPEs are often long-lasting and associated with persistent moist southerly flows. In addition, spring exhibits a secondary peak in heavy precipitation

frequency, whereas summer events are more strongly associated with localized deep convection and enhanced thermodynamic instability. Orographic lifting along the Apennines further intensifies precipitation during these events and contributes to strong spatial heterogeneity in rainfall extremes.

On the other hand, under ongoing global warming, the Emilia-Romanga region has also experienced increasingly hot summers in recent decades (Tomozeiu et al., 2006; Sabatani et al., 2024). Long-term observational datasets covering 1961–2010 reveal a significant regional warming trend, with annual mean temperatures increasing by up to approximately 0.5 °C per decade. Among these temperature-related extremes, severe heatwave events are commonly associated with persistent subtropical high-pressure systems and stagnant atmospheric conditions. The Po Valley is particularly vulnerable because of its continental characteristics, high humidity, urban heat island effects, and limited ventilation. Nighttime temperatures during heatwaves often remain elevated, increasing thermal stress on human health, infrastructure, energy demand, and agriculture.

To identify the type of extreme events most relevant to stakeholders in the Emilia-Romanga region, several discussions were conducted with **Agenzia Regionale per la Prevenzione, l'Ambiente e l'Energia dell'Emilia-Romagna (ARPAE)**, the Regional Agency for Prevention, Environment and Energy of Emilia-Romagna. Through these discussions, two major categories of climate extremes were identified as having the highest relevance and societal impacts for the region.

The first category focuses on EPEs capable of producing widespread flooding across Emilia–Romagna, particularly events associated with cut-off lows, Mediterranean cyclones, and persistent large-scale moisture transport during transition seasons such as spring and autumn. Such events have caused severe hydrological impacts in recent years, including the devastating Minerva storm in May 2023 as well as additional high-impact flooding episodes during 2024 and 2025. These events are typically characterized by sustained integrated water vapor transport, strong synoptic-scale forcing, and pronounced orographic enhancement of precipitation along the Apennines. To represent these flood-producing events within the EBD framework, daily regionally averaged accumulated rainfall was selected as the primary indicator for identifying large-scale extreme precipitation episodes over the Emilia-Romanga region.

In addition to flooding events, ARPAE emphasized the growing importance of urban heatwave conditions, particularly over the densely populated urban corridor extending across central Emilia–Romagna, including major cities such as Bologna, Modena, and Parma. Prolonged periods of extreme daytime and nighttime temperatures pose substantial risks to public health, urban infrastructure, and energy demand. Consequently, urban heatwave events were selected as the second major EBD target considered in this report for the Emilia–Romagna region.

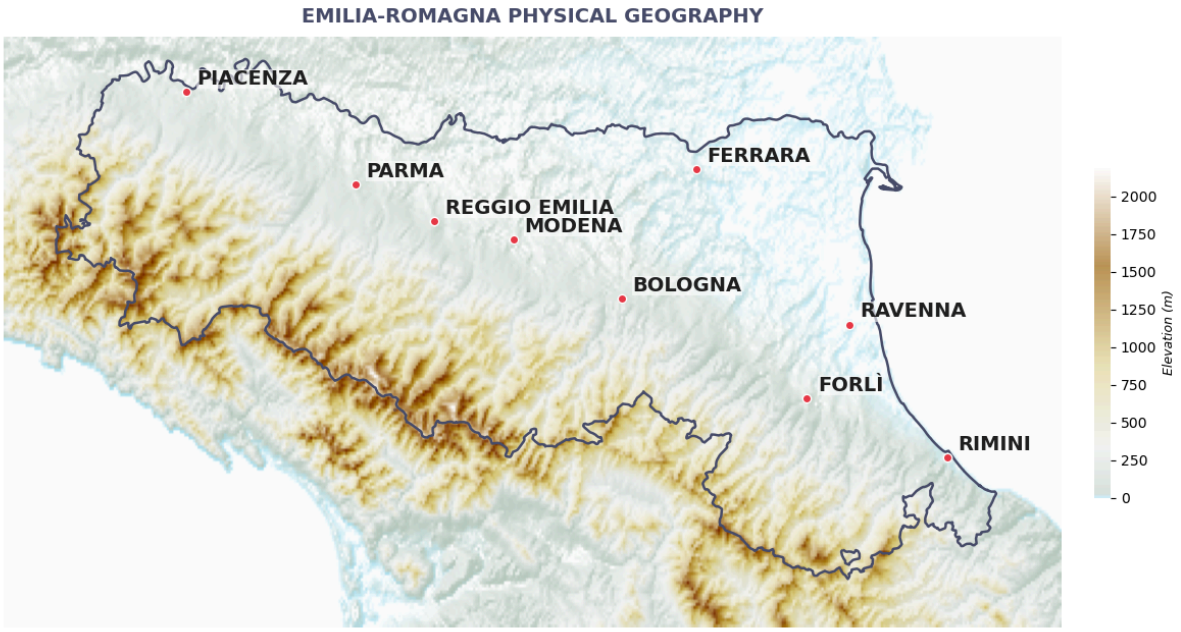


Figure 1. Topography and major cities of Emilia-Romagna. The map illustrates the regional relief using a custom terrain colormap and hillshading (azimuth 315°, altitude 60°). Data includes GMTED2010 digital elevation models (Danielson et al. 2011) and administrative borders via Natural Earth (Kelso and Patterson, 2010).

2. Methodology and data:

2.1 Data used for validation

Table 1 summarizes the datasets used for model input and validation in the EBD framework. EBD performance was evaluated using multiple observational and reanalysis datasets to assess different aspects of extreme events. Local observations ERG5 from ARPAE were used to validate regional temperature and precipitation extremes, while the E-OBS dataset provided a consistent European-scale reference for temperature and precipitation. Satellite-derived soil moisture products and the ERA5 reanalysis were used to evaluate land-surface conditions and large-scale atmospheric circulation associated with extreme events. Together, these datasets provide a comprehensive validation framework.

Table 1. Input and validation dataset used in the EBD development

Input and validation dataset used in the EBD development			
Dataset	Resolution	Purpose	Reference
ERA5 reanalysis	~31 km	Global reanalysis dataset for boundary forcing for evaluation simulations and large-scale circulation analysis	Hersbach et al. (2020)
ERG5 (Eraclito61)	5 km /	Local gridded precipitation/temperature data for event validation over Emilia–Romagna	Antolini et al. (2016)
E-OBS	10km	European wide gridded precipitation/temperature data	Cornes et al. (2018)
ESA CCI soil moisture climate data	~31 km	Soil-moisture evaluation and restoration target fields	Gruder et al. (2019)

2.1.1 Reference local data: ERG5

The Emilia-Romagna Grid 5km dataset (ERG5; Antolini et al. 2016) dataset is a high-resolution gridded meteorological and climate dataset developed by ARPAE-SIMC Emilia-Romagna. The climate version of the dataset, ERACLITO61, covers the period 1961–2010 and provides daily gridded fields of precipitation as well as minimum and maximum temperature over the Emilia-Romagna region at 5 km spatial resolution. The shorter version, ERG5, covers from 2001 to present dates with hourly temperature, precipitation, winds, and solar radiation. It is noted that the ERG5 hourly dataset has better spatial pattern accuracy in precipitation and temperature, but is not appropriate for temporal trend analysis as the station density varies with time (Arpae, 2023). Both datasets are constructed from quality-controlled station observations using topography-aware interpolation techniques specifically designed for the complex terrain of northern Italy.

In this study, we use the most recent 30-year period (1991–2023) from the ERG5 dataset to maximize the spatial coverage and consistency of the observational network, ensuring improved representation of regional precipitation and temperature variability in the evaluation of the HCLIM simulations. The observational network includes precipitation records from 254 stations and temperature records from 60 stations, which were subjected to extensive quality control, homogeneity testing, synchronicity checks, and spatial interpolation procedures. The resulting dataset provides detailed spatial representations of regional climate variability and is particularly suitable for evaluating regional climate simulations and EPEs over Emilia-Romagna.

2.1.2 E-OBS

E-OBS is a gridded observational dataset developed to provide spatially continuous climate information across Europe based on quality-controlled station observations from the European Climate Assessment & Dataset network (Cornes et al., 2018). The dataset includes daily precipitation and near-surface temperature variables and is available at a spatial resolution of 0.25° over the European continent. The dataset has been widely used for climate monitoring, model evaluation, and analyses of temperature and precipitation extremes. In this study, E-OBS is used to evaluate the spatial characteristics of summer temperature extremes over Emilia–Romagna and to provide an observational benchmark for comparison with SMHI-LENS historical simulations.

2.1.3 ESA Climate Change Initiative soil moisture climate data

The European Space Agency Climate Change Initiative (ESA-CCI) Soil Moisture dataset provides a harmonized, multi-decadal record of global surface soil moisture observations derived from a combination of active and passive microwave satellite instruments (Dorigo et al., 2017, 2019). The integration of multiple satellite products improves temporal consistency and spatial coverage, resulting in a climate data record suitable for investigating long-term hydrological variability and land–atmosphere interactions. The measurement depth depends on sensor frequency, vegetation cover, and surface conditions, but it generally corresponds to the top few centimeters of the soil, with ~2–5 cm often cited as the effective sensing depth (Dorigo et al., 2017; Gruber et al., 2019) The dataset has become a widely used reference for evaluating soil moisture variability and associated climate extremes. In this study, the ESA-CCI Soil Moisture dataset is used to assess soil moisture conditions preceding and during the heatwave events and to provide an observational reference for evaluating land-surface conditions represented in the heatwave events in the EBD framework.

2.1.4 ERA5 reanalysis

ERA5 combines a state-of-the-art numerical weather prediction system with a comprehensive data assimilation framework to provide globally consistent estimates of atmospheric, land-surface, and oceanic variables. The dataset offers continuous spatial and temporal coverage, making it particularly suitable for analysing large-scale circulation patterns, synoptic conditions, and the environmental drivers associated with regional climate

variability and extreme events. It is available at approximately 31 km horizontal resolution with hourly temporal output and includes a wide range of meteorological variables, such as near-surface air temperature, precipitation, wind, humidity, radiation, and pressure fields. Owing to its dynamically consistent representation of the climate system, ERA5 is widely used both as boundary forcing for regional climate simulations and as a benchmark dataset for model evaluation.

In this study, ERA5 serves two main purposes. First, it is used to provide the lateral boundary and initial conditions for the HCLIM dynamical downscaling simulations in evaluation mode. Second, ERA5 is employed as a reference dataset for evaluating the large-scale atmospheric conditions associated with EPEs over Emilia-Romagna. The combination of ERA5 and the high-resolution observational dataset allows for a comprehensive assessment of both the synoptic-scale environment and the regional-scale climate characteristics represented in the HCLIM simulations.

2.2 The EBD pipeline

Figure 2 provides a schematic overview of the EBD framework applied in this study. The framework is designed to investigate high-impact climate extremes by connecting large-scale atmospheric conditions from global datasets with regional- and local-scale climate information through dynamical downscaling. The procedure includes

- Definition of type of extreme event
- Detection of event in coarse resolution climate model
- Efficient spin-up of regional climate model and simulation of the event in high resolution

This procedure is automated and is carried out with hundreds of events at moderate computing costs.

In the first step, extreme events are identified from coarse-resolution datasets, including global climate model simulations and reanalysis products. Although the example shown in the figure illustrates an extreme precipitation event, the same workflow is applied to heatwave events in this study. The modular structure of the framework allows it to be adapted to different types of climate extremes while enabling event-specific definitions and detection criteria to be implemented according to the characteristics of each event type.

Following the event selection, the large-scale atmospheric conditions associated with each event are dynamically downscaled using the HARMONIE-Climate (HCLIM) regional climate model through a nested modelling strategy. Simulations are successively refined from the driving datasets at approximately 100 km resolution (or around 30 km for ERA5) to 12 km and ultimately to convection-permitting 3 km resolution. This stepwise refinement enables a more realistic representation of regional circulation features, land-atmosphere interactions, topographic effects, and mesoscale processes that are unresolved in the original large-scale

datasets. The EBD framework therefore provides a physically consistent approach for analysing how large-scale climate conditions translate into regional manifestations of extreme events across different hazard types.

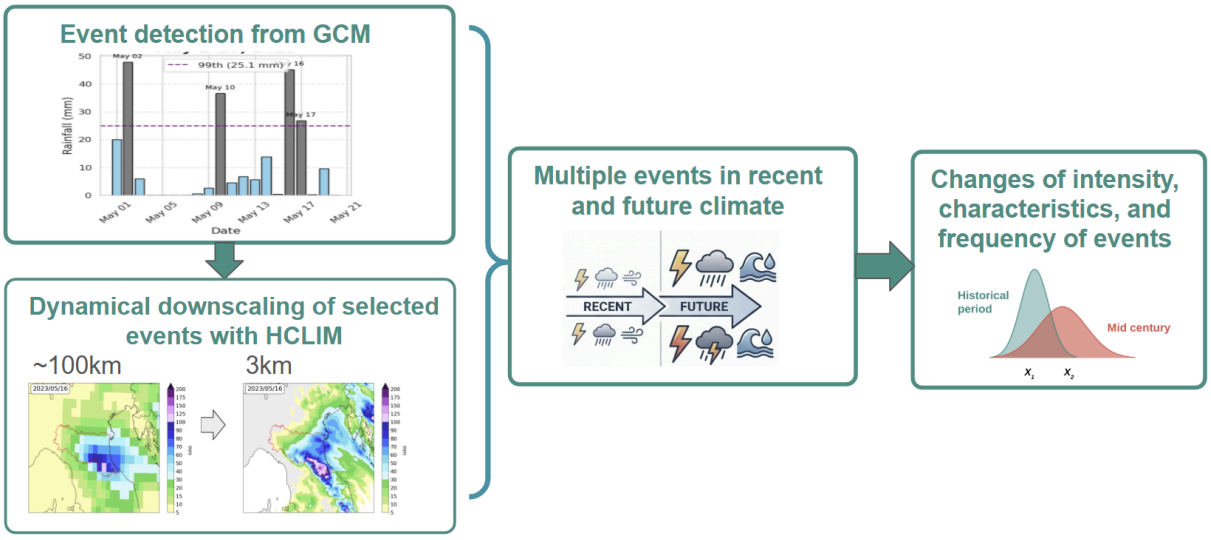


Figure 2. Schematic overview of the Event-Based Downscaling Pipeline (EBD) using the threshold-based detection method for extreme rainfall events over Emilia-Romagna.

Table 2 lists the Earth system model, SMHI-LENS, used for event detection and driving forcing for HCLIM, and regional modelling system, HCLIM, in the heart of EBD framework and the land model components and dataset used in the system.

Table 2. Models and data used in EBD framework

Models and data used in EBD framework			
Model System	Resolution	Purpose	Reference
SMHI-LENS (EC-Earth3, 50 members)	~80 km	Global climate projection for event detection and boundary forcing climate-change framework (RC and NMC)	Wyser et al. (2021)

Models and data used in EBD framework			
HCLIM v4.3	12 km / 3 km	Regional modeling system for dynamical downscaling of selected extreme events in EBD	Lindstedt et al. (2015); Belušić et al. (2020)
SURFEX v8.1	HCLIM grid	Land-surface model and soil spin-up initialization for HCLIM	Masson et al. (2013)
ECOCLIMAP-SG	~300meter	Land-cover information used in SURFEX land model for soil-moisture restoration experiments	Faroux et al. (2013)

2.2.1 Event detection strategy:

Different methods for detection of events are possible. In this project we explore two different methods for EPEs: a threshold-based method and a circulation-based method.

2.2.1.1 Threshold-based method

A threshold-based method is employed to detect both extreme rainfall and heatwave events. This approach directly uses surface variables, precipitation and temperature,as indicators of extremes. Its main advantage is the minimal data requirement, allowing consistent application across CMIP-type models, where these variables are routinely available.

Detection is based on spatially averaged variables over the Emilia-Romagna region, defined using an administrative boundary shapefile. Observational evaluation is conducted using the ERA5 reanalysis at 25 km resolution, while model-based analysis uses simulations from SMHI-LENS at 80 km resolution.

For extreme rainfall, daily accumulated precipitation is used as the detection variable. The indicator is defined as the areal-average daily rainfall over the region. All daily values across the full simulation period (100 years × 365 days) are ranked by intensity, and the top 100 events are selected as extreme rainfall cases.

For heatwaves, daily maximum temperature (Tmax) is used. A heatwave event is defined as a period of at least 7 consecutive days during which the area-average Tmax exceeds 35°C.

This definition is partly constrained by computational considerations, and can be extended based on the needs of stakeholders. Due to the coarse resolution of the SMHI-LENS model, the areal-average Tmax primarily reflects lowland conditions, with limited representation of the Apennines' topography. Nevertheless, this indicator is found to effectively capture heatwave conditions in urban areas, which is consistent with the focus of this study.

2.2.1.2 Circulation-based method

Another detection method used here, to assess the sensitivity of results against the choice of detection algorithm, is based on large-scale circulation regimes. This approach combines daily precipitation from the high-resolution Eraclito61 observational dataset (~5 km resolution; 1961–2024) with ERA5 reanalysis fields, including daily precipitation and 6-hourly 850 hPa geopotential at 0.25° resolution, to identify analogue synoptic conditions associated with heavy precipitation over Emilia–Romagna during the transition seasons (April–June and September–November). More details of this method can be found in the previous **ASPECT WP3 milestone 11.**

2.2.2 Modeling framework

2.2.2.1 HCLIM and domain setup:

The HARMONIE-Climate (HCLIM; Lindstedt et al., 2015; Belušic et al., 2020) regional climate modelling system is employed in the EBD pipeline to dynamically downscale climate conditions and extreme weather events over Emilia-Romagna. HCLIM originates from the ALADIN-HIRLAM modelling framework and is specifically developed for high-resolution regional climate applications. The land surface component of HCLIM is simulated by the SURFEX (Surface Externalisée; Masson et al., 2013) model. Subgrid surface heterogeneity is represented by four tiles, encompassing continental natural surfaces, sea, inland water and urban areas. In this project, HCLIM43 with SURFEX v8.1 is used. The experimental design adopted in this study aims to capture both the synoptic-scale circulation influencing southern Europe and the local-scale processes controlling heavy precipitation over northern Italy.

Figure 3 presents the domain configuration used for the simulations. A one-way nesting strategy is applied, consisting of an outer domain at 12 km resolution and an inner convection-permitting domain at 3 km resolution. The coarse-resolution domain spans a broad European sector and supplies the atmospheric boundary conditions to the nested simulation. The high-resolution domain covers the Alpine region and most of the Italian Peninsula, with Emilia-Romagna located well inside the interior of the domain to reduce the influence of the lateral boundaries on the analysis region. Resolving the Alpine topography within the convection-permitting domain is essential because the mountain range exerts a strong control on moisture transport and uplift mechanisms associated with intense precipitation events affecting northern Italy. Extending the high-resolution domain across the entire Alpine arc also avoids artificial discontinuities that may otherwise emerge when steep terrain intersects nested model boundaries.

Unlike the standard HCLIM configuration, where separate physical parameterization schemes are commonly applied at different horizontal resolutions, our EBD setup here uses the AROME physics package (Seity et al. 2011) in both the 12 km and 3 km domains. From previous projects, we found that applying the same physics framework across the nested configuration improves the consistency of simulated precipitation processes between scales. Earlier studies using convection-permitting HCLIM simulations have shown notable improvements in the representation of precipitation behaviour, particularly for short-duration and high-intensity rainfall, as well as for the timing of convective activity (e.g. Prein et al. 2015 and literatures within). Such improvements are especially important for Emilia-Romagna and the broader northern Italian region, where extreme precipitation is closely linked to interactions between complex terrain, moisture transport from the Mediterranean, large-scale upper-level disturbances, and convective development.

EBD simulations for method evaluation are forced by large-scale atmospheric conditions from ERA5 reanalysis and SMHI EC-Earth large ensemble integrations. Prototype simulations for assessing changing extremes were forced by CMIP6 recent climate and SSP3-7.0 simulations taken from the SMHI-LENS ESM. This setup provides a prototype framework that combines realistic large-scale circulation patterns with detailed regional-scale process representation, enabling the application of the EBD approach to generate high-resolution climate information for regional climate hazard assessment.

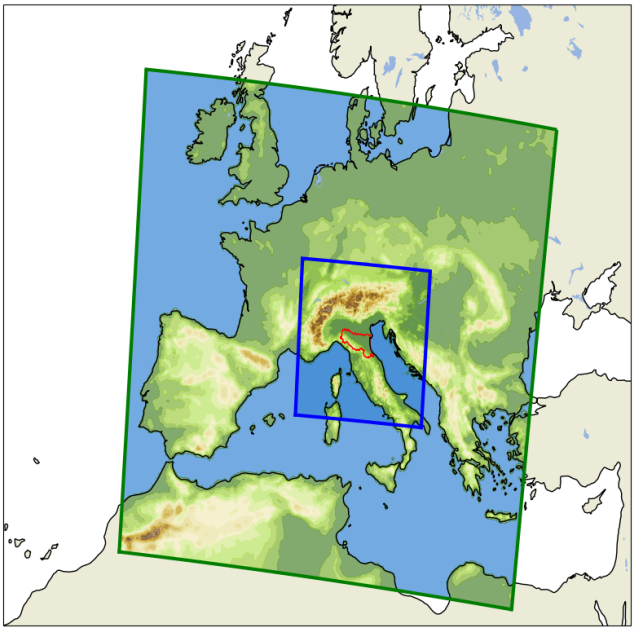


Figure 3. Model domains used for HCLIM dynamical downscaling for the Emilia-Romagna region. The green contour shows the 12 km domain, while the blue contour indicates the 3 km convection-permitting domain.

2.2.2.2 Initialization : soil spin-up procedure

When running short simulations for specific events only under the EBD (several days), a concept for computationally efficient soil spinup, with usually year-long adjustment times, needs to be developed. Here we build on the approach to speed up soil spinup procedure by running the land surface component of CPM before performing CPM simulations. Figure 4 illustrates the soil moisture content within a representative soil layer (at depth 0.5m) across three experimental setups: a long spin-up simulation (Figure 4a), the initial conditions derived from a SURFEX offline run (Figure 4b), and a cold-start configuration (Figure 4c). The results demonstrate that the method of using SURFEX offline simulation successfully establishes a soil moisture state comparable to the long spin-up case, representing a substantial improvement over the uninitialized cold start.

We evaluated several soil spin-up strategies for precipitation simulations, ranging from one day to one month before the extreme events. Sensitivity analysis demonstrated that a one-day spin-up period for both HCLIM 12km and 3km after 5-year SURFEX (land surface model) offline spinup yielded the best results compared with observational data. Consequently, 1-day initialization was applied for all simulations of precipitation events. For heatwave events simulation, we use soil moisture restoration methods.

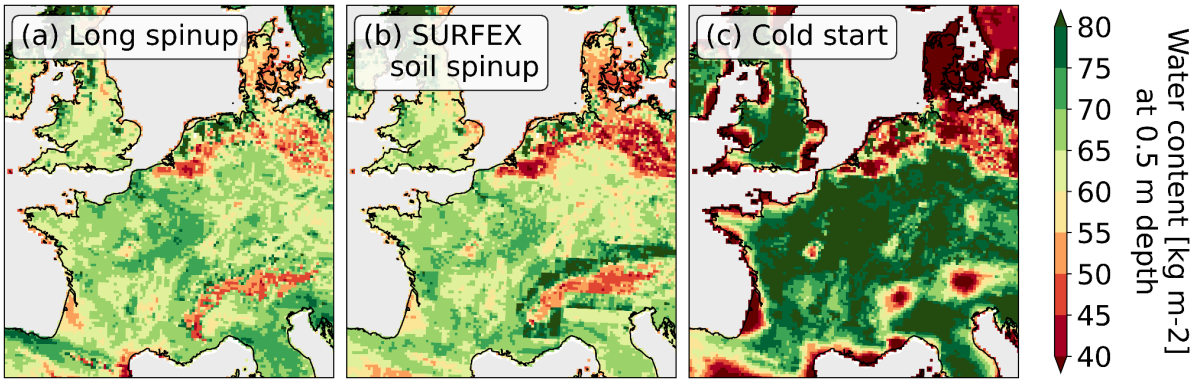


Figure 4: Example of the soil moisture at a depth of 0.5m (kg m^{-2}) for different initial condition strategies. By taking the long spinup case (a) as the reference truth, the initial condition generated by the offlineSURFEX simulation (b) provides a better spatial distribution that is more consistent than that computed from the cold start simulation (c).

2.2.2.3 Initialization : sensitivity to atmospheric spin-up initial dates

In regional climate downscaling, a spin-up period is typically required to allow the regional model to adjust from the initial and boundary conditions provided by the driving reanalysis or GCM and to develop a physically consistent internal model state. The selection of the

initialization date therefore determines the length of the spin-up period available before the target event. To evaluate the sensitivity of the HCLIM experiments to the choice of initial dates, we conducted a series of sensitivity tests using Storm Minerva (May 16, 2023) as a case study, with particular focus on the initialization and spin-up periods. The spin-up period is necessary to allow the model to develop a dynamically consistent internal state from the initial conditions provided by the reanalysis and/or GCM forcing data. For atmospheric models, a spin-up period of a few days is generally considered sufficient.

Figure 5 compares the ERA5-driven rainfall fields, local observations from ERG5, and two HCLIM simulations initialized on 14 May 2023 (Figure 5c) and 15 May 2023 (Figure 5d), respectively. The simulations were first performed on the 12-km domain and subsequently downscaled to the 3-km domain, with the event occurring on 16 May 2023. The left hand side shows the 12-km downscaled rainfall, while the right hand side shows the 3-km downscaled rainfall. The results indicate that both the initialization date and the length of the spin-up period can influence the simulated storm position. In particular, the experiment with a two-day spin-up in the 12-km domain shifted the storm further south, causing the main rainfall hotspot to occur near the southern Adriatic Sea rather than over Emilia-Romagna.

As the primary objective of this study is to accurately capture the rainfall impacts of cyclonic systems over the Emilia-Romagna region, the correct positioning of the Mediterranean cyclones is essential. To minimize positional shifts associated with longer spin-up periods, we therefore selected the configuration initialized one day before the detected event for both the 12-km and 3-km simulations.

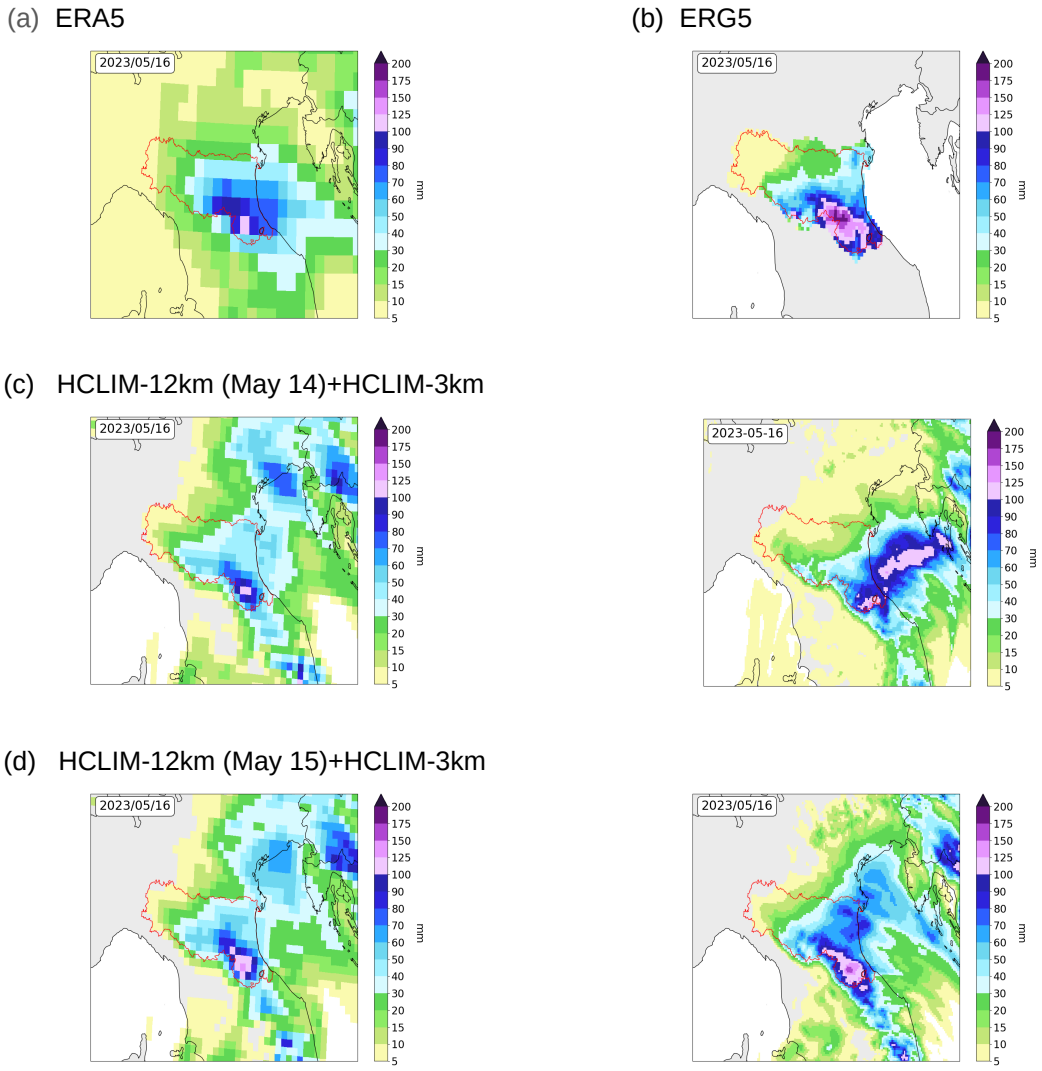


Figure 5. Sensitivity of simulated accumulated precipitation to different initial dates. Panels show precipitation distributions on May 15, 2023 from (a) ERA5 reanalysis, (b) ERG5 observational/reference dataset, (c) HCLIM simulations initialized on 14 May (12 km) and dynamically downscaled to 3 km on 15 May, and (d) HCLIM simulations initialized 15 May for both the 12 km and 3 km domains.

2.2.3 Event-specific development

2.2.3.1 Heatwave specialization: soil moisture restoration practice

Initial tests aimed at recreating past heatwave events with HCLIM43 driven by ERA5 revealed a significant dry soil bias over the Po Valley region, particularly in cropland areas. The deficit in soil moisture led to an excessive warming of near-surface air temperatures, resulting in a warm bias that became more pronounced during hotter conditions. Figure 6a compares daily maximum 2 m temperatures simulated by HCLIM at 3 km resolution with

ERG5 observations during the August 2017 heatwave. This event produced exceptionally high temperatures across southern Europe, including Italy (Di Giuseppe et al., 2017). The warm bias clearly increases with temperature, as shown by the growing deviation from the 1:1 line for the highest-temperature days (orange dots in Figure 6a).

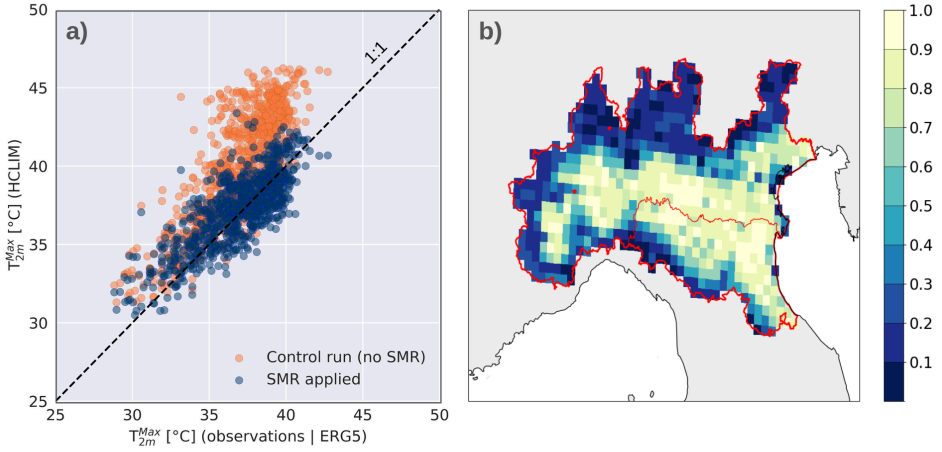


Figure 6: (a) Scatter plot of the maximum 2 metre air temperature on 4 August 2017 for the control run (orange) and with SMR applied (blue). Each point represents a 5 km grid cell over Emilia-Romagna. The HCLIM 3 km data were regridded to the ERG5 grid for comparison. (b) Fraction of grid cells covered by croplands over the Po Valley region (12 km resolution). The land cover data is retrieved from ECOCLIMAP-SG.

We further found that heatwave events were accompanied by substantial soil moisture depletion, which can amplify heatwave intensity through enhanced sensible heat flux and reduced evaporative cooling. The left panel of Figure 7 shows the near-surface soil moisture on 4 August 2017 in ESA CCI observations, indicating soil moisture values of approximately 0.25 $m^3\ m^{-3}$ across much of the Emilia–Romagna region, corresponding to relatively moist conditions close to field capacity. This contrasts with the much drier soil conditions simulated by HCLIM. The discrepancy is particularly important because Emilia–Romagna is characterized by extensive irrigated agricultural land (e.g. Villani et al. 2021), which helps maintain higher soil moisture levels during summer. To address the resulting dry soil and warm temperature biases, we developed a soil moisture restoration scheme that constrains the model soil moisture toward observed conditions during the simulation period.

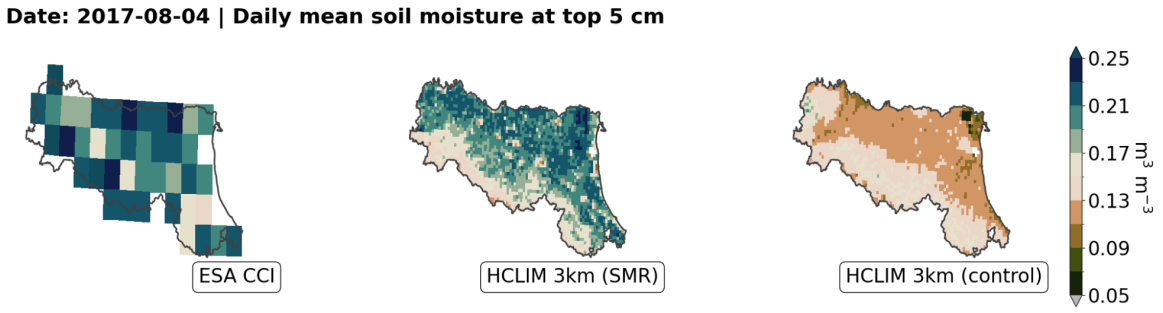


Figure 7: Daily mean soil moisture at the top 5 cm soil layer for ESA CCI, HCLIM3km-SMR, and HCLIM3km-control (from left to right) on the hottest day of the early August heatwaves in 2017.

To address the dry soil bias, we implemented a soil moisture restoration (SMR) practice. This approach involves restoring the soil moisture (W_G) in the upper 4 cm to the field capacity value (W_{FC}). In our case, the SMR was applied exclusively to croplands, as the dry soil bias was most evident in this land cover type:

$$W_G^{new}(z) = \begin{cases} f_{crop} \cdot W_{FC}(z) + (1 - f_{crop}) \cdot W_G^{old}(z), & \text{if} \quad z < 4\text{cm} \\ W_G^{old}(z), & \text{otherwise} \end{cases}$$

where f_{crop} is the fraction of the grid cell covered by croplands, see Figure 6b. The SMR correction is applied once at the beginning of each simulated day (midnight). The correction of hot and dry bias within the model is clearly seen during the heatwave day in August 2017, where correction is shown in extreme heatwave temperature (Figure 6a blue dots), and soil moisture (Figure 7 middle) during heatwaves. To further evaluate its impact, we performed simulations for the summers of 2017 and 2022, comparing the SMR runs against control runs (without SMR).

The daily average values of maximum and minimum near-surface air temperature over Emilia-Romagna, derived from HCLIM at 3 km resolution, capture the observed variability for both summers (see Figure 8). The application of SMR significantly reduces the strong warm bias in daily maximum and minimum air temperatures, aligning the simulated values more closely with observations. The dry bias in daily mean near-surface relative humidity is also improved by SMR, though the enhancement is less pronounced than for temperature.

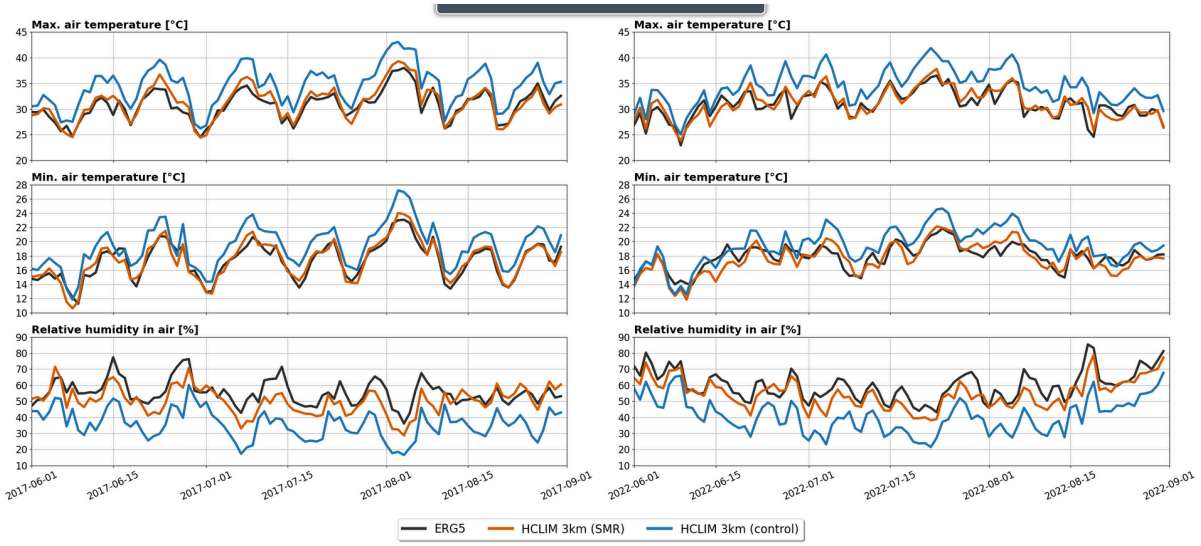


Figure 8: Daily values of (top) maximum, (middle) minimum air temperature, and (bottom) mean relative humidity. ERG5 observations (black) are compared with the control run (blue) and the run with SMR (orange) for the summers of 2017 and 2022. Simulations with SMR show improved agreement with observed values.

Spatially, the results with SMR applied are more consistent with observations, particularly over the plains, where the SMR effect is most intense (i.e., areas with a larger fraction of croplands). Figure 9 presents maps of daily maximum and minimum near-surface air temperature and mean relative humidity over Emilia-Romagna during the peak of the heatwave in early August 2017. Since SMR is not applied over urban areas, warmer values persist over cities. For relative humidity, although an underestimation remains over the plains, the values are closer to observations, and the spatial distribution better matches the observed patterns.

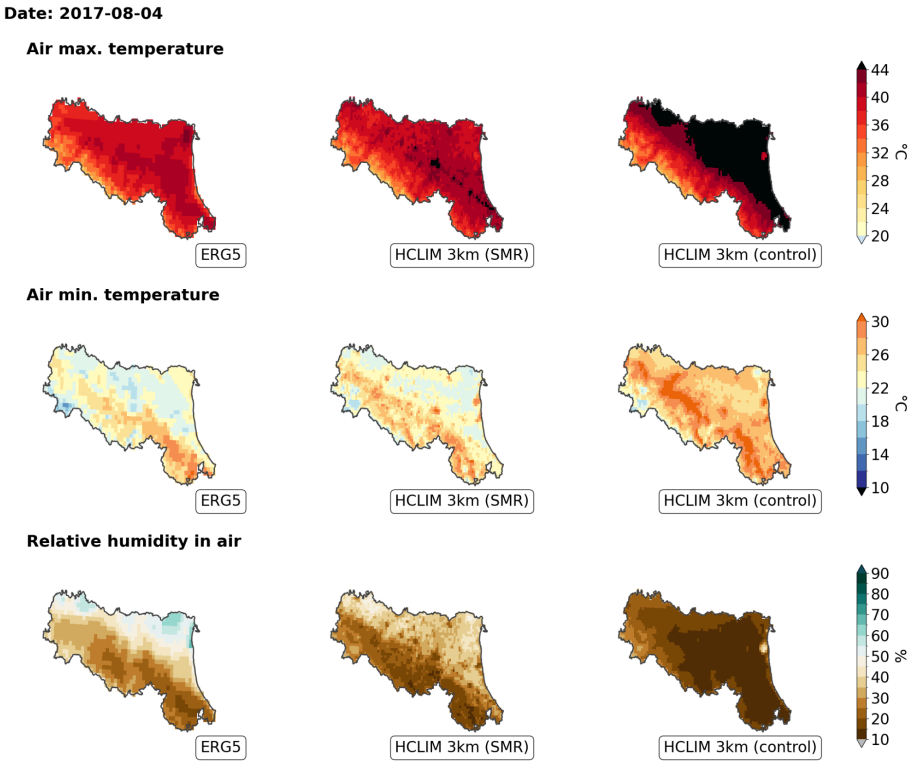


Figure 9: Spatial distribution of (top) daily maximum air temperature, (middle) daily minimum air temperature, and (bottom) mean relative humidity over Emilia-Romagna on 4 August 2017. Panels show (left) ERG5 observations, (middle) runs with SMR, and (right) control run. Simulations with SMR exhibit a closer resemblance to observations, particularly over cropland-dominated plains.

2.2.3.2 Extreme rainfall specialization: ensemble boosting

To study the uncertainty associated with precipitation events, we applied ensemble boosting to a selection of extreme cases. This statistical method involves perturbing the initial conditions of such events from an existing reference climate model simulation for each event. The goal is to generate physically consistent trajectories of very rare extremes, as illustrated in Figure 10.

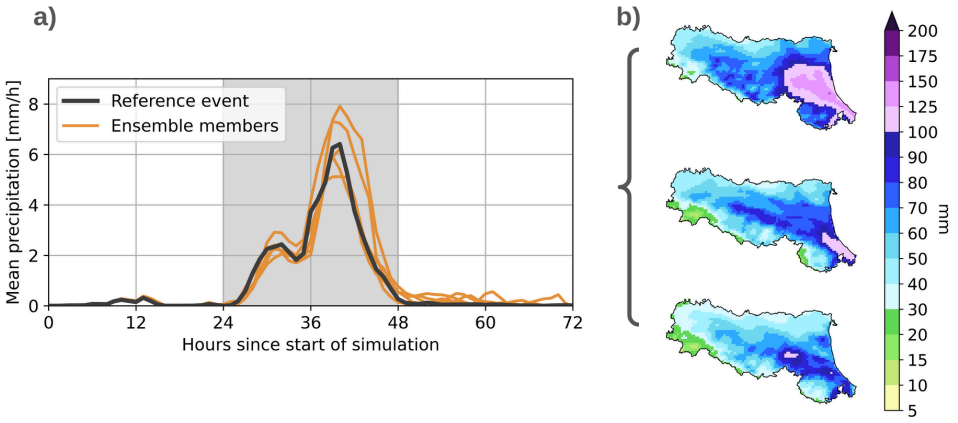


Figure 10: (a) Example of the ensemble boosting application. The orange lines depict multiple realisations of a single event, with each ensemble member starting from a perturbed version of the reference simulation's initial condition (black). (b) Precipitation accumulation (hours 24–48) for a selection of ensemble members, showing spatial rainfall distribution sensitivity to initial perturbations.

Our approach follows the methodology outlined by Bloin-Wibe et al. (2025), in which the initial specific humidity field, Q^{def}, is perturbed using the following equation:

$$Q^{modi}(x, y, z) = Q^{def}(x, y, z)(1 + 10^{-13}R(x, y, z))$$

Here, R represents a random term drawn from a uniform distribution between -0.5 and 0.5. In our simulations, the ensemble boosting is applied to the intermediate nest simulation at 12 km resolution.

2.3 30-year prediction framework with SMHI-LENS

Figure 11 shows the framework of evaluation and climate change frameworks used with the EBD pipeline. For model evaluation and model setup, we have used the ERA5 reanalysis to provide boundary forcing of HCLIM. For the climate change framework, we have used a large ensemble from a CMIP6 model, the SMHI large ensemble (SMHI-LENS) based on 50 ensemble members from EC-Earth (Wyser et al. 2021).

As illustrated in the right-hand panel of Figure 11, the climate change–impact study framework is based on a CMIP6 Large Ensemble (SMHI-LENS; Wyser et al., 2021), generated with EC-Earth3.

The SMHI-LENS consists of 50 realizations spanning 1970–2100 and was developed to quantify the role of internal climate variability in future climate evolution and extreme events. All ensemble members are forced with the same external radiative forcing, while differences between members arise from perturbed initial atmospheric and oceanic conditions. To construct the ensemble, six EC-Earth3 historical simulations were used as parent runs, from

which additional 20-year “breeding” simulations with fixed forcing were initialized in 1970. Different states sampled from these breeding simulations were then used to initialize the 50 ensemble members, providing multiple physically consistent realizations of climate evolution under the same external forcing.

To embed climate-change information within the seamless prediction framework in ASPECT, we compare the **Recent Climate (RC)** around the year 2000 with the **Near Mid-Century Climate (NMC)** around the year 2040, providing an approximately 30-year climate prediction horizon. In SMHI-LENS, the **RC** corresponds to climate conditions around the year 2000, which approximately coincide with the **0.9°C global warming level**, whereas the **NMC** represents climate conditions around 2040 and corresponds to the **2.0°C global warming level** under the SSP3-7.0 scenario. This framework enables a consistent comparison of extreme-event characteristics across different climate states while maintaining a seamless prediction perspective (Figure 11).For each of the 50 ensemble members, the year at which the global mean temperature first reaches the target warming level was identified. A 2-year time slice window centred on this crossing year was then extracted from each member. Combining the 2-year periods from all 50 members yields approximately 100 model years for each warming level, thereby providing a sufficiently large sample for robust extreme-event statistics while still preserving the thermodynamic characteristics associated with the selected warming level. The same methodology was applied consistently for both the 0.9°C and 2.0°C climates.

The resulting 100-year datasets were subsequently analysed using the event-detection methodology developed for the EBD catalogue. The detection framework follows the philosophy used in previous studies of extreme precipitation over northern Italy, where large samples of events are extracted and classified using objective detection approaches and environmental diagnostics . This approach enables a consistent comparison between historical and future climates, while explicitly accounting for the contribution of internal variability through the large-ensemble framework.

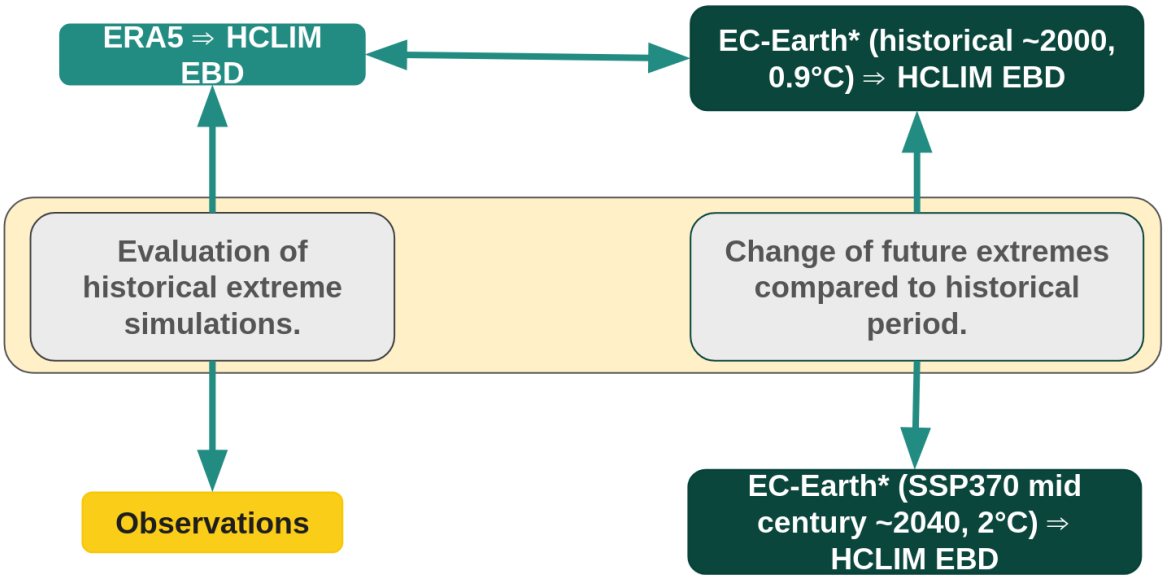


Figure 11. Schematic overview of the methodology used for the evaluation and climate impact analysis of the EBD experiments. ERA5-driven HCLIM simulations are used to evaluate historical extreme events against observational datasets, while SMHI-LENS-driven HCLIM simulations are used to assess future changes in extreme events by comparing the Recent Climate (~2000, corresponding to a 0.9°C global warming level) and the Near Mid-century Climate (~2040, corresponding to a 2°C warming level) climate conditions. The warming levels are selected from the SSP3-7.0 scenario of the SMHI Large Ensemble (SMHI-LENS; Wyser et al., 2021). For each ensemble member, two years are selected for the extreme-event analysis, resulting in a total of 100 model years used for event selection and climate impact assessment.

2.4 Extreme event analysis

To quantify the statistical rarity of extreme precipitation represented in the EBD catalogue, a Generalized Extreme Value (GEV; Cole 2001) analysis was applied to the dynamically downscaled EPEs. According to extreme value theory, the distribution of sufficiently large block maxima converges asymptotically to the GEV distribution (Cole 2001). Let X1,X2,...,Xn denote the sequence of annual or event-based precipitation maxima extracted from the EBD catalogue. These maxima are treated as independent realizations of a random variable X, whose cumulative distribution function is approximated by the GEV distribution G(z), such that:

$$P(X \leq z) = G(z)$$

where G(z) describes the probability that the event maximum precipitation does not exceed a threshold z.

These samples are assumed to be realizations drawn from an underlying extreme-value distribution. The GEV fitting procedure estimates the parameters (μ,σ,ξ) such that the distribution G(z) best represents the statistical behavior of the observed maxima Xi, where μ

is the location parameter, σ>0 is the scale parameter, and ξ is the shape parameter controlling the upper-tail behavior of the distribution.

The fitted GEV distribution allows estimation of exceedance probabilities and return periods for simulated precipitation extremes. The return period (T) associated with a precipitation intensity (zT) is defined as:

$$T = \frac{1}{1-G(zT)}$$

To quantify sampling uncertainty associated with the limited number of EBD events, a bootstrap resampling approach was additionally applied (Efron and Tibshiran, 1993). A total of 1000 bootstrap subsamples were generated by random resampling with replacement from the original EBD event catalogue. The GEV fitting procedure was repeated independently for each bootstrap sample, producing an ensemble of estimated return levels and cumulative distribution functions. The spread among these bootstrap realizations was then used to estimate the uncertainty range of the fitted extremes, and the 2.5th–97.5th percentile interval from the bootstrap ensemble was adopted as the corresponding 95% confidence range.

The bootstrap-based uncertainty estimation is particularly important for the EBD framework because the catalogue contains only a limited number of dynamically selected extreme events. Consequently, estimates of very high return periods are sensitive to the sampling of a few upper-tail events and to the fitted GEV shape parameter. The resulting return statistics should therefore be interpreted as event-conditioned estimates derived from physically plausible extreme-event realizations, rather than as definitive stationary climatological return values from continuous long-term simulations. Nevertheless, the combined EBD–GEV framework provides a physically consistent approach for translating dynamically downscaled extreme-event simulations into probabilistic risk metrics such as exceedance probability, return level, and associated uncertainty ranges.

3. Description of the event catalogue

3.1 Catalogue architecture

The catalogue comprises a total of 530 extreme events, including 400 EPEs and 130 heatwave events. Event numbers of rainfall and heatwave extreme events are provided in Table 3.

Table 3. Event numbers of extreme events catalogue

Number of extreme events in the catalogue		
Methods	**Recent Climate (~Year 2000)**	**Near Mid-century (~Year 2040)**
Rainfall with threshold-based detection	100	100
Rainfall with circulation-based detection	100	100
Heatwave with soil moisture restoration	31	99

The catalogue is organised hierarchically according to the type of extreme event and the associated warming level scenario. At the first level, the events are divided into two main categories: heatwaves and EPEs. Within each category, the events are further subdivided into historical events, corresponding to the RC scenario, and future events, corresponding to the NMC scenario, as illustrated in Figure 12. Each directory then contains the individual simulated events. The variables contained in each event can be found in Table S2 and S3.

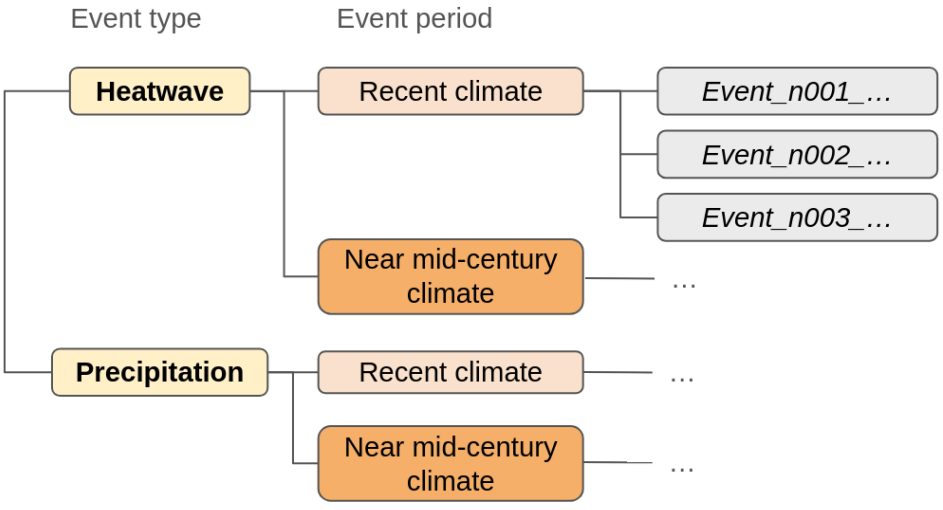


Figure 12: Schematic overview of the hierarchical organization of the EBD catalogue. The catalogue is organised first by event type (EPEs and heatwaves), then by warming level (Recent Climate, RC; Near Mid-century Climate, NMC), followed by individual event directories containing the corresponding simulation output and metadata.

For each event type, an index file is provided containing the main metadata associated with the simulations. This includes the event number, the selected SMHI-LENS ensemble member, the HCLIM realisation, and the start and end dates of the simulation period. In addition, the file reports the mean and maximum intensity of each event over Emilia-Romagna, expressed as *pr* for EPEs and as *tasmax/tasmin* for heatwave events.

Each event is identified according to the following naming convention:

Event_n<*NN*>_**r**<*RRR*>**-m**<*MM*>_<*Start-date*>**-**<*End-date*>

where <*NN*> denotes the event number, <*RRR*> corresponds to the SMHI-LENS realisation member, and <*MM*> identifies the HCLIM realisation member. Finally, <*Start-date*>**-**<*End-date*> correspond to the beginning and end of the simulated period, respectively. It should be noted that the simulated period is generally longer than the duration of the extreme event itself.

3.2 Event selection criteria

Different event-selection approaches were applied for EPEs and heatwave events in order to account for their distinct temporal characteristics and physical mechanisms.

For EPEs, the two detection methods mentioned in 2.1.1 were applied within the EC-Earth simulations to identify high-impact regional rainfall events over Emilia–Romagna. Both methods were designed to focus on **daily large-scale precipitation extremes affecting the entire Emilia–Romagna region**, but they employed different detection strategies to assess the robustness and sensitivity of the event selection. Following the detection procedure, all identified events were ranked according to the magnitude of the regional-average rainfall intensity, and the 100 strongest events were selected for the EBD precipitation-event catalogue. For each selected event, a 6-day simulation window was constructed, consisting of a 1-day spin-up period prior to the identified peak event day followed by the subsequent event evolution. This setup allows the dynamical downscaling simulations to adequately develop the mesoscale atmospheric structures and precipitation processes associated with the extreme events. Additionally, to better represent the uncertainty associated with convective processes during intense EPEs, ensemble-boosting simulations were performed within the HCLIM EBD framework. Three representative events from each detection method were selected for 5-member ensemble simulations, resulting in a final set of five independent EPE cases after removing overlapping events identified by both detection approaches.

For heatwave events, a persistence-based detection approach was adopted to represent prolonged urban heat-stress conditions during the summer season. The initial event detection was performed using area-averaged daily maximum temperature (Tmax) over the Emilia–Romagna region from the SMHI-LENS simulations. **Heatwave episodes were identified when elevated Tmax conditions persisted for at least seven consecutive days**, thereby targeting sustained heatwave conditions rather than isolated hot days. The detected events were subsequently dynamically downscaled using the HCLIM EBD framework and included in the event catalogue. For the detailed analysis presented in this

report, the downscaled events were further post-filtered using the Bologna region as a representative urban-impact area. Only events maintaining at least seven consecutive days of elevated Tmax conditions over the Bologna area were retained for analysis. This additional filtering step ensures that the final heatwave cases specifically represent persistent urban heatwave conditions affecting the densely populated Emilia corridor.

3.3 Data format and variables

All model output is provided in NetCDF format and CMORised according to the EURO-CORDEX CMIP6 archiving specifications and metadata conventions. HCLIM generates a wide range of output variables; however, for the purposes of this deliverable, a subset of 20 key variables has been selected, primarily based on the CORDEX core variable list which is considered most relevant for impact applications. The variable table can be found in Supplementary Materials attached at the end of this synthesis report.

Due to the large volume of generated data, the CMORised dataset has been spatially cropped to the Emilia-Romagna region in order to reduce storage requirements and improve data accessibility. Upon request, selected variables may also be provided for the original full model domain.

4. Evaluation & performance

4.1 Extreme rainfall analysis:

4.1.1 Validation of rainfall spectrum in SMHI-LENS Recent Climate and ERG5

Figure 13 compares the regional-average rainfall characteristics between the observational ERG5 dataset and the SMHI-LENS simulations over Emilia–Romagna, focusing on the rainfall histogram (Figure 13a,b) and the seasonal occurrence of EPEs exceeding the 99th percentile threshold (Figure 13c,d). Overall, the SMHI-LENS simulations reproduce the main statistical characteristics of the observed rainfall distribution reasonably well. Both datasets exhibit a strongly right-skewed rainfall spectrum, characterized by a large number of low-intensity rainfall events and a progressively decreasing frequency toward higher rainfall intensities. The percentile thresholds derived from the two datasets are also very similar, with the 90th percentile corresponding to 7.85 mm day^{-1} in ERG5 and 7.20 mm day^{-1} in SMHI-LENS, the 95th percentile to 12.80 and 11.32 mm day^{-1}, respectively, and the 99th percentile to 25.05 and 21.17 mm day^{-1}. This agreement indicates that the large-scale precipitation climatology represented by SMHI-LENS is broadly consistent with the observational reference and is suitable for threshold-based event detection within the EBD framework.

Some differences nevertheless emerge in the upper tail of the rainfall distribution. ERG5 exhibits a heavier tail, with several rare events exceeding 40 mm day^{-1} and a maximum

regional-average rainfall approaching 50 mm day^{-1}. In contrast, the SMHI-LENS distribution shows a smoother decline in event frequency and a slightly lower 99th-percentile threshold, suggesting a tendency to underestimate the intensity of the most extreme regional precipitation events. Such differences are expected given the coarser spatial resolution of the driving climate simulations and the limited ability of global climate models to fully represent localized heavy-rainfall processes.

The seasonal occurrence of 99th-percentile EPEs is also realistically represented by SMHI-LENS (Figure 13c,d). Both datasets show a pronounced seasonal cycle, with extreme events occurring throughout the year but becoming substantially more frequent during late summer and autumn. In ERG5, the highest occurrence is found in October, followed by November and September, while SMHI-LENS exhibits a very similar seasonal structure with a clear maximum in October and elevated frequencies during September and November. Both datasets also indicate a secondary enhancement during late spring and early summer, particularly in May and June. This seasonal behaviour is consistent with the known climatology of extreme precipitation over northern Italy, where enhanced Mediterranean moisture availability and favourable large-scale circulation patterns contribute to frequent autumn flooding events.

Although some differences remain in the intensity of the most EPEs and in the month-to-month occurrence frequencies, the SMHI-LENS simulations successfully reproduce both the overall rainfall spectrum and the seasonal evolution of regional precipitation extremes over Emilia–Romagna. This agreement provides confidence that the EBD framework, when applied to SMHI-LENS simulations, is able to identify physically plausible extreme precipitation events that are suitable for subsequent dynamical downscaling.

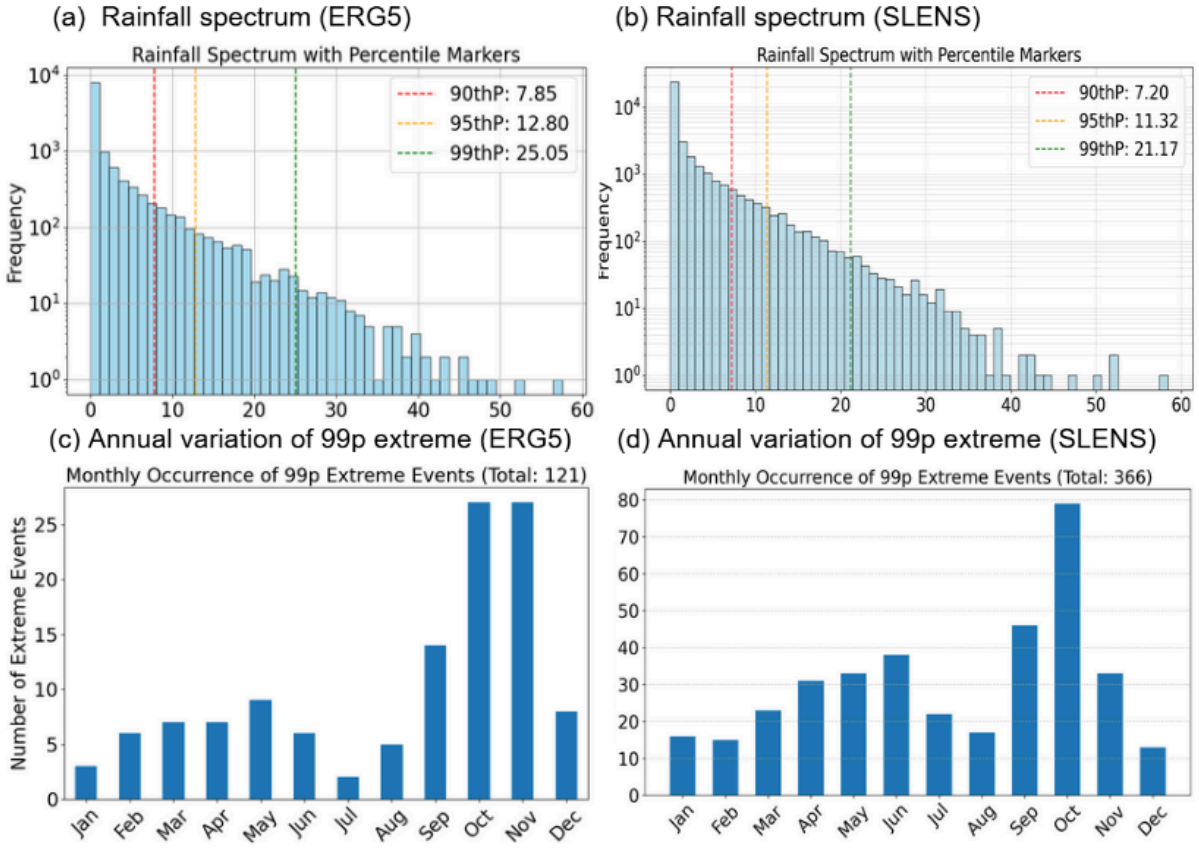


Figure 13. Comparison of regional-average daily rainfall characteristics over the Emilia–Romagna region between the observational ERG5 dataset and the SMHI-LENS simulations. (a) Rainfall spectrum derived from ERG5 together with the 90th, 95th, and 99th percentile thresholds. Blue vertical lines indicate selected high-impact extreme precipitation events. (b) Same as (a), but for the SMHI-LENS. (c) Monthly occurrence of regional extreme precipitation events exceeding the 99th percentile threshold in ERG5. (d) Same as (c), but for the SMHI-LENS.

4.1.2 Validation of intensity statistics in EBD-SMHI-LENS Recent Climate

To assess the realism of the EBD framework in representing extreme precipitation over Emilia-Romanga, the rainfall characteristics of the dynamically downscaled EBD simulations are compared with both the driving SMHI-LENS simulations and the high-resolution observational dataset ERG5. The analysis evaluates the extent to which the convection-permitting HCLIM simulations improve the representation of the magnitude and variability of regional extreme precipitation relative to the coarse-resolution global model, particularly for localized high-intensity rainfall associated with mesoscale and convective processes. This comparison therefore provides an assessment of the added value of dynamical downscaling for reproducing event-scale precipitation extremes over the Emilia-Romanga region.

Figure 14 presents the distribution of event area maximum rainfall from SMHI-LENS, HCLIM-12km, HCLIM-3km, and ERG5 for the 100 selected EPEs. SMHI-LENS exhibits a

relatively narrow distribution with systematically lower rainfall intensities, indicating that the coarse-resolution global model strongly smooths localized precipitation extremes. In contrast, both HCLIM-12km and HCLIM-3km produce substantially broader distributions and enhanced upper-tail variability, reflecting their improved representation of mesoscale dynamics and convective precipitation processes. The convection-permitting simulations reproduce numerous events exceeding 150–200 mm day−1, with several events approaching the intensity range represented in the ERG5 observations. HCLIM-3km further exhibits slightly larger upper-tail extremes and greater variability than HCLIM-12km, suggesting that the finer-resolution configuration provides additional capability for resolving localized intense precipitation structures. Although the EBD simulations still underestimate the most extreme rainfall maxima represented in ERG5, they reproduce the overall intensity distribution and variability substantially better than the driving SMHI-LENS simulations. It should also be noted that the EBD rainfall characteristics are influenced by the event-selection methodology, since the 100 EBD events are identified using the coarse model-based detection framework and therefore do not necessarily correspond to the most EPEs contained within the ERG5 observational dataset.

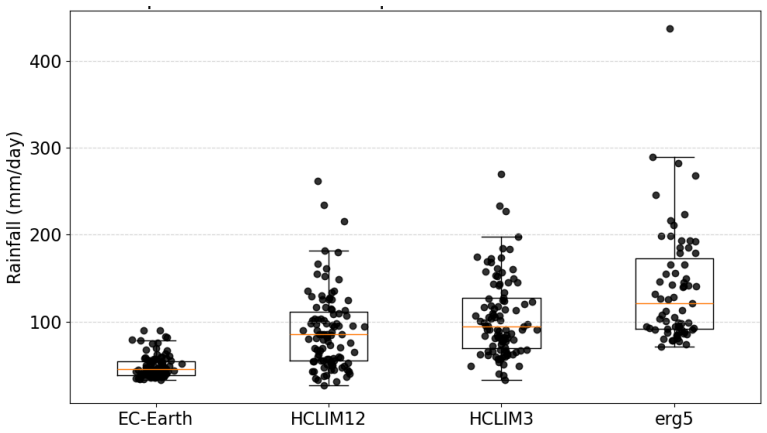


Figure 14. Distribution of event maximum areal rainfall for the 100 selected extreme precipitation events over the Emilia–Romagna (ER) region from the driving SMHI-LENS simulations, the EBD downscaled HCLIM-12km and HCLIM-3km simulations, and the high-resolution observational ERG5 dataset. Events are selected based on the area mean rainfall over the ER region. Boxplots indicate the median, interquartile range, and overall spread of event rainfall intensity, while dots represent individual extreme precipitation events.

4.1.3 Validation with large-scale circulation related to EPE in Recent Climate

To assess whether the combination of SMHI-LENS and the EBD detection framework is able to identify physically realistic extreme events with large-scale dynamical structures comparable to those found in observations and reanalysis datasets, we have conducted composite of large-scale circulation patterns associated with the 20 EBD EPEs selected from the SMHI Large Ensemble at RC using the threshold-based method.

We found that the composed large-scale circulation is generally consistent with the synoptic characteristics reported in previous studies of observed EPEs over northern Italy and the broader Emilia-Romanga region. The 500-hPa geopotential height anomaly composite (Figure 15a) shows a pronounced negative anomaly centered over the western–central Mediterranean, indicating the presence of a deep upper-level trough extending southward from western Europe toward Italy. This configuration resembles the canonical Rossby-wave and PV-streamer patterns frequently associated with Mediterranean heavy precipitation events, where amplified upper-level troughs enhance large-scale ascent and promote strong meridional moisture transport toward northern Italy (Grazzini et al., 2020a, 2021). Similar synoptic precursors have also been linked to warm conveyor belts and atmospheric rivers affecting the Po Valley and southern Alpine slopes, which are known to favor widespread heavy precipitation events over northern Italy (Pfahl et al., 2014; Raveh-Rubin and Wernli, 2015).

The sea-level pressure anomaly composite (Figure 15b) further reveals a well-defined cyclonic pressure anomaly over the central Mediterranean and northern Italy, consistent with the development of Mediterranean cyclogenesis or lee cyclones near the Gulf of Genoa–Adriatic region. Such circulation patterns favor enhanced low-level southerly to southeasterly moisture transport from the Mediterranean Sea toward the Apennines and Alpine foothills, which has been widely recognized as a key mechanism for triggering heavy precipitation events in northern Italy (Massacand et al., 1998; Davolio et al., 2016; Miglietta and Davolio, 2022). Previous studies have further demonstrated that these environments are commonly associated with strong integrated water vapor transport and moisture convergence over the Emilia-Romanga region (Grazzini et al., 2020a, 2021).

Overall, the close agreement between the RC composite structures and the large-scale dynamical features documented in observational and reanalysis-based studies indicates that the SMHI-LENS combined with the EBD detection framework is capable of successfully identifying physically consistent EPEs. The reproduced upper-level trough and surface cyclonic circulation patterns suggest that the selected RC events capture the key synoptic-scale processes responsible for high-impact precipitation over Emilia–Romagna region.

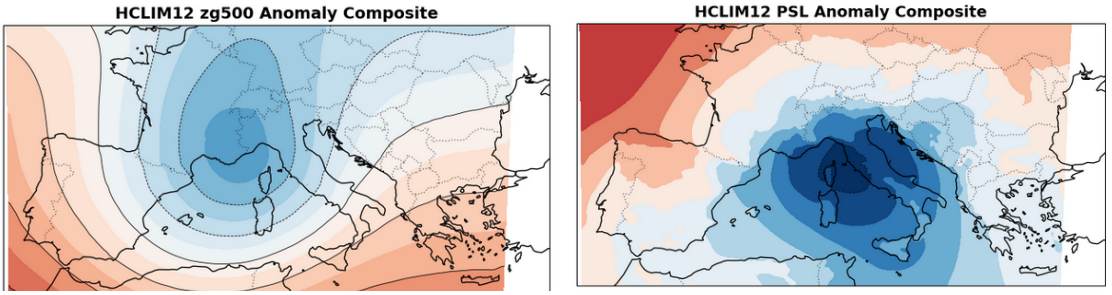


Figure 15. Composite of spatial anomalies of large-scale circulation fields associated with the 20 extreme precipitation events selected from the SMHI Large Ensemble at RC using the threshold-based EBD detection method. The areal average is computed over the HCLIM-12km domain. (a) 500-hPa geopotential height anomalies and (b) sea-level pressure anomalies derived from HCLIM-12km simulations. Blue shading indicates negative anomalies and red shading indicates positive anomalies.

4.2 Heatwave analysis :

This section presents evaluations of two key components of the summer heatwave analysis within the EBD framework: the representation of high-percentile Tmax in the SMHI-LENS/EC-Earth simulations and the heatwave event characteristics in the convection-permitting EBD downscaled simulations.

4.2.1 Validation of Tmax statistics in SMHI-LENS in Recent Climate

Figure 16 compares the spatial distribution and statistical characteristics of summer 90th percentile daily maximum temperature (90p Tmax) between the observational E-OBS/ERG5 datasets and the EC-Earth-based SMHI-LENS simulations under the recent climate (RC) over Emilia–Romagna. The observational dataset shows a pronounced topographic contrast, with substantially lower 90p Tmax values over the Apennines and Alpine regions due to elevation-induced cooling effects, while the highest temperatures exceeding 35 °C are concentrated along the central and eastern lowland sectors of the Emilia plain. In contrast, the SMHI-LENS simulations reproduce the broad lowland warm corridor and the general occurrence of 35 °C conditions over the Emilia plain, but the topographic cooling signal is much weaker. As a result, the model substantially overestimates 90p Tmax over the Apennines and Alpine areas and only partially resolves the spatial extent of the warmest lowland core. This behavior is consistent with the relatively coarse resolution of SMHI-LENS, which cannot adequately capture the strong terrain-induced thermal gradients characteristic of northern Italy.

The quantile–quantile analysis over the Emilia–Romagna plain region (10.5–12.8°E, 44.6–45.15°N) in Figure 15c further demonstrates that both the EC-Earth historical simulations and the SMHI-LENS RC simulations exhibit very similar statistical characteristics relative to the ERG5 observations. The models reproduce the observed Tmax distribution reasonably well for temperatures around 32 °C, indicating that the large-scale thermal

conditions over the lowlands are realistically represented. However, both EC-Earth and SMHI-LENS show a systematic warm bias in the upper tail of the distribution, particularly above approximately the 85th percentile and for temperatures exceeding 35 °C. The magnitude of this bias is relatively moderate, generally around 1–2 °C, but indicates that the models tend to overestimate the frequency and intensity of the hottest summer days. Importantly, the close agreement between the historical EC-Earth and SMHI-LENS simulations suggests that the ensemble framework preserves the same large-scale temperature characteristics as the driving global model.

These results suggest that SMHI-LENS is capable of reproducing the large-scale warming features and extreme heat characteristics over the Emilia–Romagna lowlands. However, the model is less able to resolve the strong thermal contrasts associated with the Apennine and Alpine topography. This supports the use of SMHI-LENS threshold-based detection methods for identifying heatwave events primarily over the lowland regions, where the large-scale temperature distributions are more realistically represented. In this study, the 90th percentile Tmax metric is additionally selected because it closely corresponds to the operational 35 °C heatwave threshold adopted by ARPAE for regional heat-warning applications.

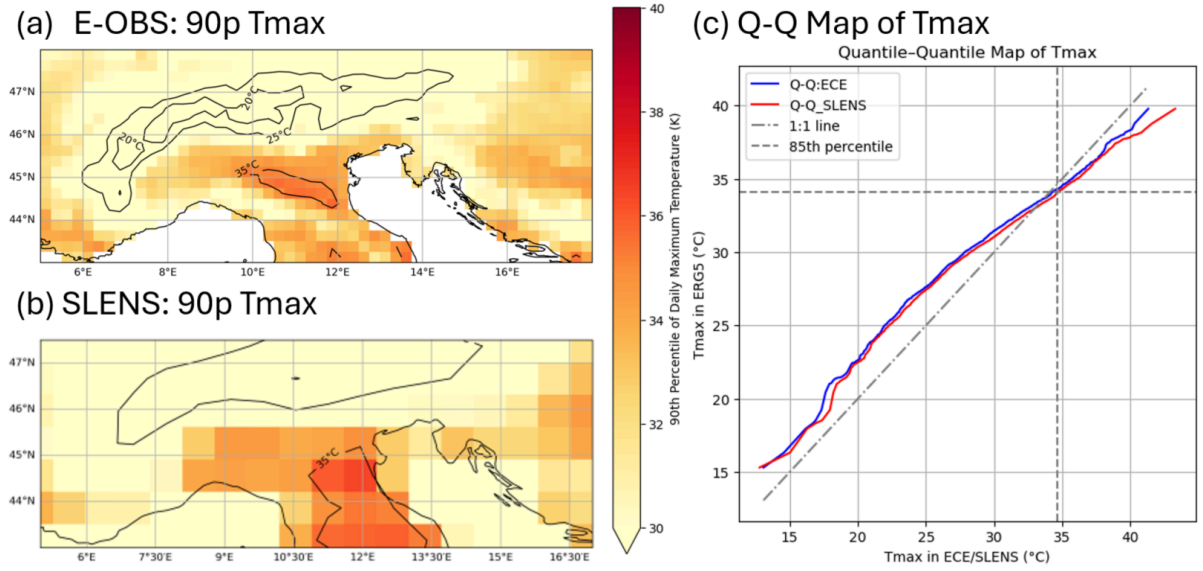


Figure 16. Comparison of summer (JJA) extreme daily maximum temperature characteristics over the Emilia–Romagna region between observations and EC-Earth/SMHI-LENS simulations. (a) Spatial distribution of the 90th percentile daily maximum temperature (90p Tmax) from the observational E-OBS dataset, and (b) corresponding 90p Tmax from the SMHI-LENS RC simulations. Contours indicate selected temperature thresholds highlighting 20°C, 25°C, and 35°C. (c) Quantile–quantile (Q–Q) comparison between Tmax distributions from ERG5 observations averaged over the Emilia–Romagna plain region (10.5–12.8°E, 44.6–45.15°N) and Tmax from the EC-Earth historical and SMHI-LENS simulations averaged over the entire Emilia–Romagna domain. The dashed horizontal and vertical lines indicate the 85th percentile threshold, approximately corresponding to the 35 °C threshold.

4.2.2 Validation of heatwave events in EBD-SMHI-LENS in Recent Climate

Based on the Bologna-centered heatwave events identified in the EBD framework, where heatwaves are defined as periods with at least seven consecutive days of Tmax exceeding 35 °C over the Bologna region, we compare the spatial characteristics of both daytime and nighttime heatwave durations against the observational ERG5 dataset.

Figure 17 presents the spatial distribution of daytime heatwave duration, defined as the number of days with Tmax exceeding 35 °C during the selected heatwave episodes, from the EBD-SMHI-LENS RC simulations and the ERG5 observations. For the daytime heatwave characteristics, the EBD simulations generally reproduce the major spatial patterns of observed heatwave conditions across the region, although some regional discrepancies remain (Figure 17a). Both datasets indicate that the most persistent daytime heatwave conditions are concentrated over the lowland and urbanized sectors of the Po Valley, particularly along the Bologna–Modena–Reggio Emilia corridor, while substantially fewer extreme hot days occur over the Apennine mountain regions. This pronounced spatial contrast highlights the important role of topography and land-surface characteristics in modulating regional heat stress over Emilia–Romagna.

Compared with ERG5, the EBD simulations capture the large-scale spatial gradient between the cooler mountainous areas and the hotter lowland regions reasonably well. Especially over the cities around Bologna and adjacent urbanized regions, EBD simulations produce very strong contrast between the urban environment and the low plains. These differences likely reflect the model resolution and the representation of local land–atmosphere interactions and urban effects within the regional climate simulations. Nevertheless, the EBD framework successfully reproduces the dominant spatial characteristics of prolonged daytime heat stress events over Emilia–Romagna.

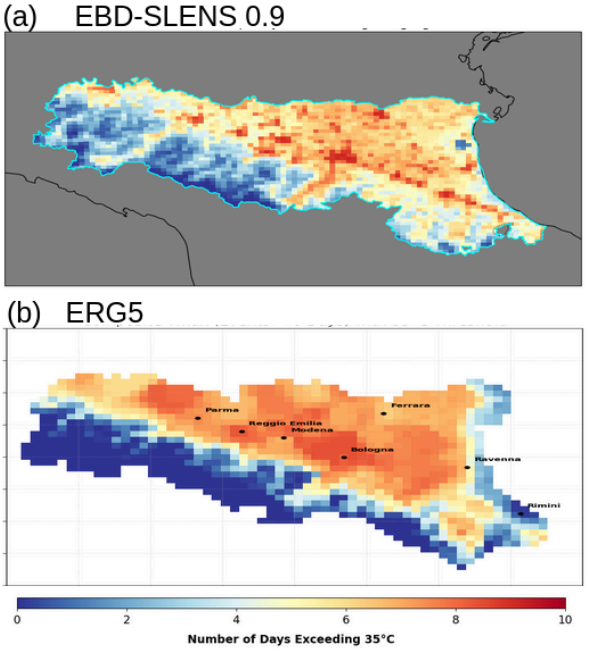


Figure 17. Spatial distribution of daytime heatwave durations, defined using maximum temperature (Tmax), over the Emilia–Romagna region from (a) the EBD-SMHI-LENS 0.9 simulation and (b) the observational ERG5 dataset. Colors indicate the duration of daytime heatwaves with days with Tmax exceeding 35 °C, representing extreme daytime heat conditions associated with thermal stress.

Figure 18 shows the duration of tropical nights during the same heatwave events, defined as days with Tmin exceeding 20 °C. The nighttime heatwave characteristics exhibit a distinctly different spatial structure compared with the daytime Tmax extremes. The EBD simulations are able to reproduce the general spatial organization of nocturnal heat stress, including the stronger nighttime heatwave persistence over the plains relative to the mountainous regions (Figure 18a). However, compared with the ERG5 observations (Figure 18b), the simulations again show a smoother spatial structure and weaker localization of urban hotspots. The observed Tmin extremes exhibit stronger small-scale variability, especially around Bologna and coastal areas, while the simulated fields display broader regional patterns. Despite these differences, the EBD simulations capture the overall enhancement of nighttime heatwave duration over the Po Valley and the reduction over elevated terrain, indicating that the dynamical downscaling framework provides a physically consistent representation of both daytime and nighttime heatwave characteristics during persistent extreme heat events over Emilia–Romagna.

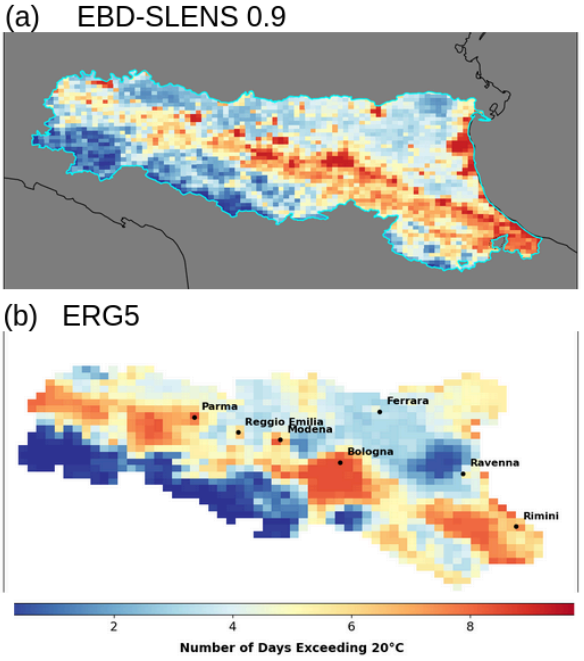


Figure 18. Spatial distribution of nighttime heatwave durations, defined using minimum temperature (Tmin), over the Emilia–Romagna region from (a) the EBD-SMHI-LENS 0.9 simulation and (b) the observational ERG5 dataset. Colors indicate the duration of nighttime heatwaves with days with Tmin exceeding 20 °C, representing tropical nights associated with nocturnal heat stress.

5. Uncertainty & methodology constraints

Although previous analysis has demonstrated that the Event-Based Downscaling (EBD) framework provides a practical approach for generating high-resolution climate information on extremes, the resulting projections remain subject to uncertainties arising from multiple components of the modelling chain. These uncertainties originate from the large-scale driving data, event selection methodology, regional climate model configuration, and the limited sampling of rare extreme events. In addition, the prototype nature of the current framework and the finite size of the available event catalogue introduce further constraints on the robustness of the projected changes. Understanding these limitations is essential for interpreting the results presented in this report and for guiding future developments of the EBD framework. The following sections discuss the principal sources of uncertainty and their implications for the interpretation of the generated event catalogue.

5.1 GCM and scenario dependency

One important source of uncertainty in the current EBD framework for estimating future changes in extreme events over the Emilia-Romanga region is the reliance on a single global climate model (GCM) to provide the lateral boundary conditions for the dynamical downscaling. Although we performed a careful evaluation of the SMHI-LENS large ensemble in representing regional rainfall and temperature extremes, the present study does not account for inter-model uncertainty in future projections. Previous studies have highlighted that the choice of driving GCM can substantially influence the performance and outcomes of regional climate model (RCM) simulations, particularly for precipitation extremes and circulation-dependent processes (e.g. Sobolowski et al. 2025). The representation of large-scale circulation patterns, moisture transport, and thermodynamic conditions associated with EPEs may vary considerably among GCMs, thereby affecting the downscaled regional responses. For example, studies over northern Italy have demonstrated the important role of large-scale dynamical precursors, including Rossby wave packets and integrated water vapour transport, in shaping extreme precipitation characteristics (Grazzini et al., 2020a, 2021). Different GCMs may reproduce these large-scale processes with varying fidelity, which introduces additional uncertainty into the EBD projections.

In addition, our analysis is limited to a single future forcing scenario (SSP3-7.0) derived from SMHI-LENS. Different socioeconomic pathways and greenhouse gas emission trajectories can lead to substantially different regional climate responses, especially for temperature-related extremes and hydrological intensification. Therefore, the projected changes presented here should be interpreted as scenario-specific rather than comprehensive estimates of future uncertainty. The method development in ASPECT provided a prototype application and demonstrates the potential for broader use across ESMs and regions. The prototype is applicable to other CMIP GCMs, especially those who provide input to CORDEX downscaling, which is the base of many climate change services in Europe.

5.2 Detection sensitivity

As a key component of the EBD framework, the event detection methodology plays a critical role in determining how extreme events are sampled from the driving GCM simulations and therefore directly affects the overall performance and efficiency of the EBD pipeline. Different detection approaches may preferentially identify events with distinct physical characteristics, leading to differences in the sampled event distributions and associated climate statistics. To provide an assessment of the uncertainty associated with event detection in the EBD framework, we applied two different detection approaches in this study: **a circulation-based method** and **a threshold-based method**.

To assess the sampling characteristics of the EBD catalogues, Figure 19 shows the annual exceedance rate as a function of rainfall intensity. For a rainfall threshold p, the exceedance probability is defined as

$$P(X > p) = \frac{N\ (X>p)}{N_{years}},$$

where N(X>p) is the number of events exceeding p, and N is the total number of samples. For ERG5, which is a continuous daily record during 1991–2023, the annual exceedance rate is calculated as

$$R_{ERG5}(p) = \frac{N_{days}(X>p)}{N_{years}},$$

where $N_{years} = 33$. For the EBD catalogues, which consist of selected events from 100 model years, the annual exceedance rate is estimated as

$$R_{EBD}(p) = \lambda_{EBD} P_{EBD}(X > p)$$

where

$$\lambda_{EBD} = \frac{N_{events}}{N_{years}}$$

is the event occurrence frequency and $N_{years} = 100$.

The exceedance-rate ratio shown in Figure 19b is defined as

$$Q(p) = \frac{R_{EBD}(p)}{R_{ERG5}(p)}$$

where values of Q(p)<1 indicate that the EBD catalogue underestimates the occurrence frequency of rainfall events above threshold p, while Q(p)>1 indicates overestimation.

Both EBD catalogues show substantially lower annual exceedance rates than ERG5 across a wide range of rainfall intensities (Figure 19a). This behaviour reflects the design of the EBD framework, which targets extreme precipitation events rather than the full spectrum of daily weather conditions. For example, the exceedance rate in ERG5 decreases from approximately 1–2 events yr−1 at 20 mm day−1 to about 0.1 events yr−1 at 40 mm day−1, corresponding to a return period of roughly 10 years. In contrast, both EBD catalogues exhibit exceedance rates below 0.03 events yr−1 at 40 mm day−1, more than an order of magnitude lower than the ERG5 reference. Consequently, the exceedance-rate ratio remains below 0.2 for both methods at moderate rainfall thresholds, and falls below 0.1 for the circulation-based method over much of the 20–50 mm day−1 range. These results indicate that both detection approaches substantially under-sample moderate and relatively frequent precipitation events.

For rainfall intensities exceeding approximately 40 mm day−1, corresponding to events with return periods of about 5–10 years in ERG5, differences between the two detection approaches become more apparent. The threshold-based catalogue consistently exhibits higher exceedance rates than the circulation-based catalogue and approaches the ERG5 reference more closely. At rainfall thresholds above approximately 60 mm day−1, the exceedance-rate ratio of the threshold-based method approaches unity and even exceeds it for the most extreme events, whereas the circulation-based method remains below unity across all thresholds. It is also noteworthy that 18 events are simultaneously identified by both detection methods, and all overlapping cases belong to the most extreme subset within the combined event catalogue. This indicates that, despite methodological differences, the two approaches consistently identify the highest-impact extreme rainfall events. The differences between the resulting distributions highlight the sensitivity of the EBD framework to the event-detection methodology and demonstrate that event selection constitutes an important source of uncertainty in event-based climate assessments. Overall, the results demonstrate that both detection methods successfully identify high-impact precipitation events suitable for EBD downscaling, but they also share a common limitation. Because both approaches are designed to target extreme precipitation episodes, they substantially undersample weaker and more frequent rainfall events, particularly those below approximately the ERG5 1-year return level. As a result, neither method should be expected to reproduce the full climatological rainfall distribution. Instead, both approaches preferentially sample the upper tail of the precipitation spectrum, consistent with the objective of constructing an event-focused catalogue of high-impact extremes.

For the present Emilia–Romagna prototype application, where the primary objective is to sample the most intense regional precipitation extremes, the threshold-based approach may offer a practical advantage. However, this finding should be interpreted with caution. The relative performance of the two methods is likely influenced by the characteristics of the selected event type, the regional climate, the driving climate model, and the specific detection criteria employed. The threshold-based method preferentially selects events associated with high precipitation intensities in the driving model, whereas the circulation-based method samples events based on physically relevant large-scale atmospheric conditions. Consequently, the two approaches should be viewed as

complementary rather than competing methodologies, each emphasizing different aspects of extreme-event behaviour. Further evaluation using larger event samples, alternative climate models, different hazard types, and other geographical regions is required to assess the robustness and broader applicability of these findings.

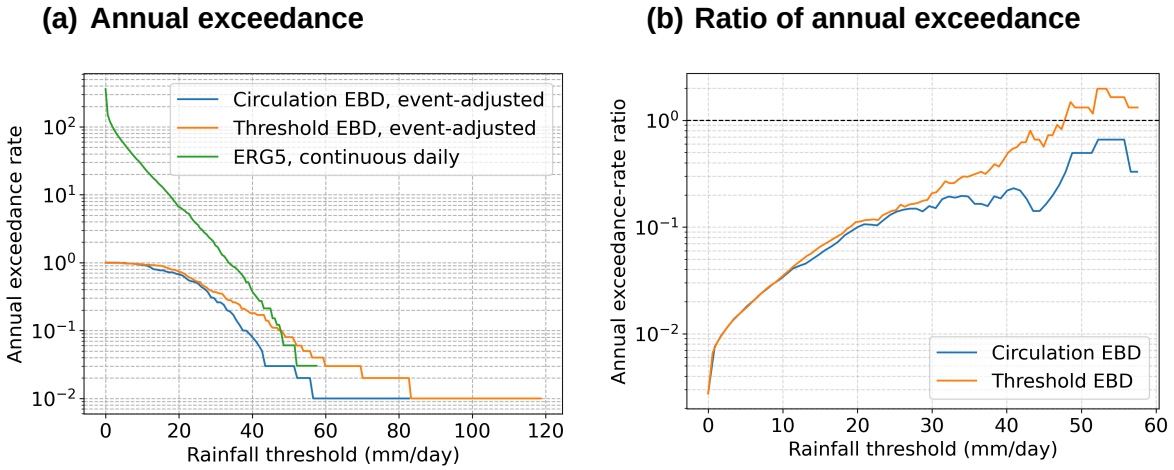


Figure 19. Event-adjusted exceedance frequency of regional-average rainfall and corresponding exceedance-rate ratios for ERG5 and the two EBD approaches. (a) Annual exceedance rate as a function of rainfall threshold for ERG5 (green), circulation-based EBD (blue), and threshold-based EBD (orange). ERG5 rates were calculated from the continuous daily record during 1991–2023, while exceedance rates for the EBD catalogues were adjusted by the event occurrence frequency in the 100-year catalogue (λ=Nevents/Nyears) to obtain annual exceedance rates. (b) Ratio of annual exceedance rates between the EBD simulations and ERG5. Values below unity indicate that the EBD catalogue underestimates the frequency of rainfall events relative to ERG5, while values above unity indicate overestimation.

5.3 Initialization Risks

Unlike continuous regional climate downscaling simulations, in which the atmospheric and land-surface states evolve continuously and remain dynamically consistent throughout the simulation period, the EBD framework is inherently constrained by the initialization procedure for individual events. Each EBD simulation is initialized from parent GCM conditions with a relatively short spin-up period, which may lead to inconsistencies between the initial atmospheric and land-surface states and the internal physics of the RCM. Such initialization imbalances can introduce additional uncertainty into the representation of precipitation extremes, particularly for convective processes and land–atmosphere interactions that are highly sensitive to soil moisture, boundary-layer evolution, and mesoscale circulation adjustments.

In this study, we found that the offline soil spin-up has mixed impacts on extreme event simulations over the Emilia-Romanga region. While the preconditioning of soil moisture before the rainfall event, applying offline soil moisture actually amplifies existing soil moisture biases over the Emilia-Romanga region, an issue that has already been recognized within the HCLIM community. Because soil moisture strongly regulates surface heat and moisture fluxes, biases in land-surface initialization can substantially influence the development and persistence of heatwave events. In particular, dry soil conditions can suppress evapotranspiration and enhance sensible heat fluxes, leading to stronger near-surface warming and reinforcing positive land–atmosphere feedbacks that favor heatwave intensification. Therefore, uncertainties associated with soil initialization may significantly affect the simulated magnitude, duration, and spatial extent of extreme temperature events in the EBD framework.

Therefore, the results from this project highlight that careful initialization practices are crucial for the EBD pipeline. In particular, maintaining consistency between atmospheric forcing, land-surface states, and RCM physics is essential to reduce artificial adjustment processes during the early simulation period. Future work should further investigate the sensitivity of EBD simulations to spin-up length, soil moisture initialization strategies, and land-surface parameterizations in order to improve the robustness of convection-permitting simulations of EPEs.

6. Synthesis: future climate signals

6.1 Rainfall dynamics

6.1.1 Event changes in extremes with percentile method

Figure 20 compares the annual exceedance rates between the Recent Climate (RC) and Near Mid-century Climate (NMC) simulations for the threshold-based and circulation-based EBD catalogues. For the **threshold-based** detection method (Figure 20a), the annual exceedance-rate curves are nearly identical over rainfall thresholds below approximately 40 mm day−1, indicating that the frequency of moderate extreme events remains largely unchanged between the two climate states. Differences emerge only in the upper tail of the distribution, where RC exhibits slightly higher exceedance rates than NMC for rainfall thresholds exceeding approximately 60 mm day−1. This suggests a modest reduction in the occurrence of the most intense regional-average rainfall events under the NMC, although the differences remain small and are limited to the rarest events.

For the **circulation-based** detection method (Figure 20b), the climate-change signal differs slightly. While the overall distributions remain similar, NMC exhibits consistently higher exceedance rates than RC for rainfall thresholds between approximately 35 and 60 mm day−1, indicating a slight increase in the occurrence of moderate-to-strong extreme

precipitation events. However, this difference disappears for the highest rainfall thresholds, where the two climate states converge and RC retains marginally higher exceedance rates for the most extreme events. Compared with the threshold-based method, the circulation-based approach therefore suggests a somewhat stronger increase in moderate extremes while showing little evidence for changes in the most severe regional-average precipitation events.

Overall, both detection methods indicate that changes in the exceedance characteristics of regional-average rainfall between RC and NMC are relatively modest over the approximately 30-year prediction horizon considered in this study. However, the sign and magnitude of the projected changes vary with the event-selection strategy, particularly for moderate-to-strong rainfall intensities. This sensitivity demonstrates that conclusions regarding future changes in extreme precipitation are not independent of the detection methodology. Because threshold-based and circulation-based approaches emphasize different aspects of extreme-event behaviour—local rainfall intensity versus favourable large-scale atmospheric circulation—they sample different subsets of events from the same climate simulation. Consequently, the interpretation of projected changes in extreme rainfall frequency should consider the uncertainties introduced by the event-selection methodology in addition to those arising from the climate simulations themselves.

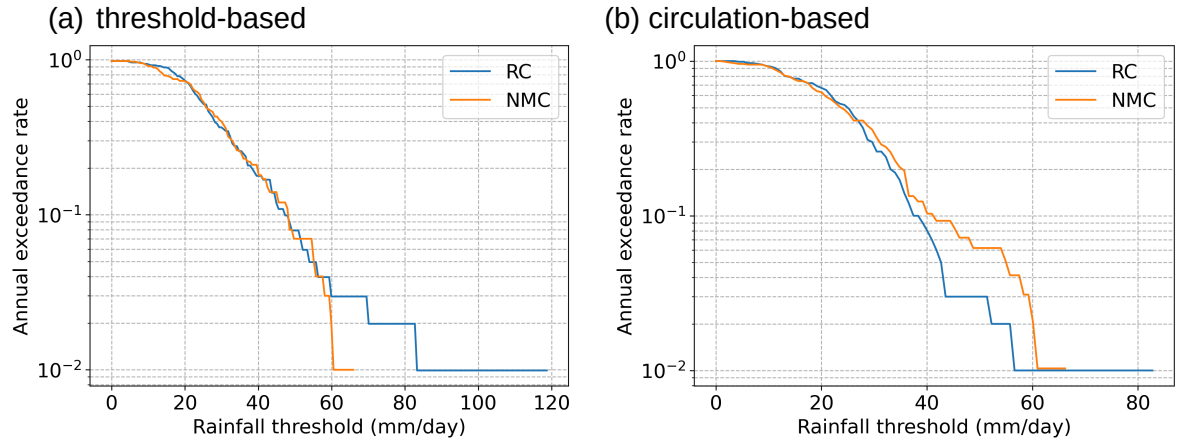


Figure 20. Annual exceedance rate of regional-average rainfall for the (a) threshold-based and (b) circulation-based EBD catalogues under the Recent Climate and Near Mid-century Climate simulations. Annual exceedance rates were calculated by multiplying the exceedance probability by the event occurrence frequency within each 100-year catalogue. Values on the y-axis represent the average number of events per year exceeding a given rainfall threshold.

6.1.2 Event Changes with Generalized Extreme Value Estimation

Here, we only applied the GEV to the EPEs with a threshold-based method, as it provides more intense EPEs, and shows better consistent with ERG5. For each detected EPE, the

event maximum precipitation over Emilia–Romagna was extracted from the convection-permitting HCLIM simulations. Since the EBD framework selects approximately one representative extreme event per simulated model year, the resulting set of event maxima can be interpreted analogously to an annual maximum series. The extracted maxima were therefore used within a block-maxima extreme value framework to estimate the statistical distribution of rare precipitation extremes.

Figure 21 compares the precipitation return levels derived from the EBD catalogue under RC and NMC conditions for both the convection-permitting EBD simulations and the driving SMHI-LENS simulations. The results show that the response to warming is qualitatively similar in EBD and SMHI-LENS. In both datasets, RC exhibits lower return levels than NMC at longer return periods, indicating a reduction in the most EPEs under the mid-century climate conditions represented by the selected EBD events. This behavior is consistent with the earlier analyses of event-frequency distributions, which showed a decrease in the occurrence of the most severe rainfall events under warming. This also suggests that the EBD methodology reproduces events that follow the frequency changes within its driving GCM.

While the climate-change signal is consistent between EBD and SMHI-LENS, substantial differences are evident in the magnitude of the simulated precipitation extremes. Across the entire return-period range, EBD produces considerably larger precipitation intensities than SMHI-LENS, with the differences becoming increasingly pronounced toward the upper tail of the distribution. This amplification reflects the added value of convection-permitting downscaling, which explicitly resolves mesoscale and convective precipitation processes that are largely parameterized in the coarse-resolution global model. Consequently, the EBD simulations produce rainfall intensities that are much closer to those observed in the ERG5 dataset as demonstrated in the previous validation analyses.

The EBD simulations indicate that the most EPEs are generally stronger under RC than under NMC, particularly for return periods exceeding approximately 20–30 years. The divergence between the two climate states becomes increasingly pronounced toward the upper tail of the distribution, suggesting a reduction in the occurrence of the most severe precipitation events within the EBD catalogue under warmer conditions.

However, this result is associated with substantial uncertainty, particularly for the rarest events where only a limited number of samples are available. The confidence intervals increase rapidly with return period, reflecting the limited number of EBD events available to constrain the fitted GEV distributions. Consequently, estimates of precipitation extremes at return periods exceeding approximately 100 years are subject to considerable sampling uncertainty and should be interpreted with caution.

The apparent tendency towards weaker regional-scale extremes under NMC may at first seem inconsistent with the succession of exceptionally severe rainfall events that have affected Emilia–Romagna in recent years, including the catastrophic floods of May 2023 and October 2024 (e.g. Coppola et al. 2024). However, caution is required when interpreting

these EBD projections in the context of individual observed events. High-impact precipitation events arise from a combination of anthropogenic warming, internal climate variability, and favourable large-scale atmospheric circulation. As a result, individual events do not necessarily reflect the long-term forced climate response, because internal climate variability can temporarily mask or outweigh the anthropogenic signal. This effect is particularly important for the relatively short (~30-year) prediction horizon considered in this study, during which externally forced changes are expected to remain comparable to, or even smaller than, the magnitude of natural climate variability.

This interpretation is consistent with previous regional climate projection studies. EURO-CORDEX simulations show that projected changes in heavy precipitation over northern Italy and the western Mediterranean remain weak and are generally indistinguishable from internal climate variability during the mid-century, in contrast to the more robust increases projected by the end of the century (Coppola et al., 2021).

Moreover, previous studies suggest that the relatively weak mid-century response results from the competing influences of thermodynamic and dynamical processes. A warmer atmosphere increases moisture availability and enhances the potential intensity of heavy precipitation through the Clausius–Clapeyron relationship. At the same time, several studies project changes in the large-scale circulation over the Mediterranean, including a reduction in the frequency of Mediterranean cyclones, a poleward shift of the North Atlantic jet stream (e.g. Doensen et al., 2026), and a decline in the occurrence of western Mediterranean cut-off lows, which are closely associated with many high-impact rainfall events over northern Italy (Misha et al., 2025). However, these circulation changes exhibit substantial inter-model spread and pronounced multi-decadal variability, making the forced dynamical response difficult to distinguish from natural variability over the mid-century period (Brajkovic et al., 2026). Consequently, thermodynamic intensification may be partly offset by uncertain dynamical changes, resulting in relatively modest changes in regional precipitation extremes.

Within this context, and considering the uncertainties associated with the EBD framework discussed in Section 5, further research is required to determine whether the relatively modest differences between the RC and NMC climates identified in this study represent a robust physical response or arise primarily from internal climate variability and sampling uncertainty. In particular, a more comprehensive assessment should account for uncertainties associated with climate model diversity and internal variability by applying the EBD framework to multiple GCMs and large ensembles. This is especially important because the frequency and characteristics of EBD-selected events are closely linked to the large-scale circulation simulated by the driving GCM. Nevertheless, despite these uncertainties, the EBD framework provides an efficient and physically consistent approach for generating targeted convection-permitting simulations of high-impact events. By enabling computationally affordable large ensembles of event-based simulations, EBD offers a practical framework for assessing future changes in extreme-event characteristics while explicitly accounting for multiple sources of uncertainty.

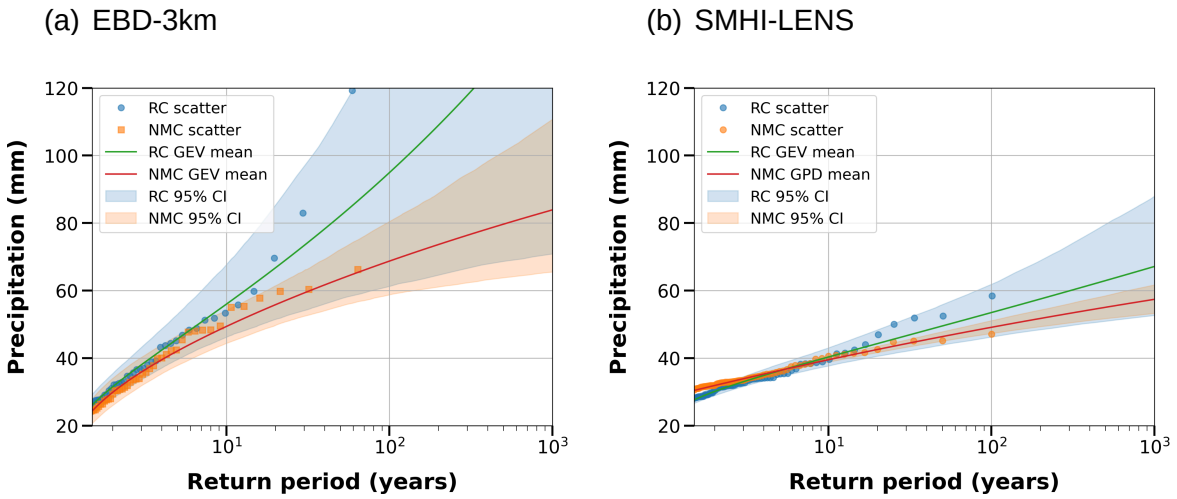


Figure 21. Return-level estimates of daily precipitation derived from simulations for recent climate conditions (RC) and Near Mid-century Climate (NMC). Results are shown for (a) EBD convection-permitting simulations and (b) the driving SMHI-LENS simulations. Symbols indicate empirical return levels derived from the EBD event samples, while solid lines represent the fitted Generalized Extreme Value distributions. Shaded areas denote the 95% confidence intervals estimated from 1000 bootstrap resamples. Return periods are calculated based on the 100-event EBD catalogue. Blue and orange colors correspond to RC and NMC, respectively.

6.2 Heatwave Dynamics

6.2.1 Changes of heatwave events characteristics over hot days

Based on the heatwave definition used in this study, events are identified as periods of at least 7 consecutive days with daily maximum temperature exceeding 35 °C. Using the SMHI-LENS simulations, 31 heatwave events are detected within the 100 simulated years under RC, compared with 99 events under NMC. For the EBD application, the 99 events are subsequently post-processed according to the event-selection criteria, resulting in 80 independent heatwave events for downscaling and further analysis. The substantial increase in event occurrence under NMC indicates a strong rise in the frequency of extreme heat conditions and represents the main driver of the projected increase in heatwave impacts over Emilia–Romagna.

Figure 22 further illustrates the associated changes in heatwave characteristics between the two warming levels. Figure 22a shows the annual changes in heatwave days associated with the detected events. A widespread increase in annual heatwave days is identified across nearly the entire Emilia–Romagna region, with the strongest increases occurring over the central and eastern lowland areas, including the Po Valley and the urbanized surroundings of

Bologna. The projected increase generally ranges between approximately 2 and 4 additional heatwave days per year, whereas comparatively weaker changes are found over the western mountainous regions. The spatial distribution suggests enhanced sensitivity of low-elevation inland areas to future warming, likely associated with stronger land–atmosphere feedbacks, reduced nocturnal cooling efficiency, and urban heat island effects that favor the persistence of warm conditions.

In comparison, Figure 22b indicates that projected changes in heatwave intensity, defined here as the mean Tmax averaged across all detected heatwave events, exhibit a spatially homogeneous but comparatively moderate positive signal across the Emilia–Romagna region. Although increases in event intensity are evident throughout the domain, the magnitude of warming generally ranges from approximately 0.5 °C to locally about 1 °C, which remains relatively weak compared to the substantial increase in annual heatwave occurrence. This suggests that future warming primarily manifests through a higher frequency and persistence of heatwave events rather than through a strong amplification of peak event intensity. Nevertheless, the coherent positive anomalies across the region indicate an overall enhancement of thermal stress under the warmer climate state, particularly over densely populated and urbanized areas.

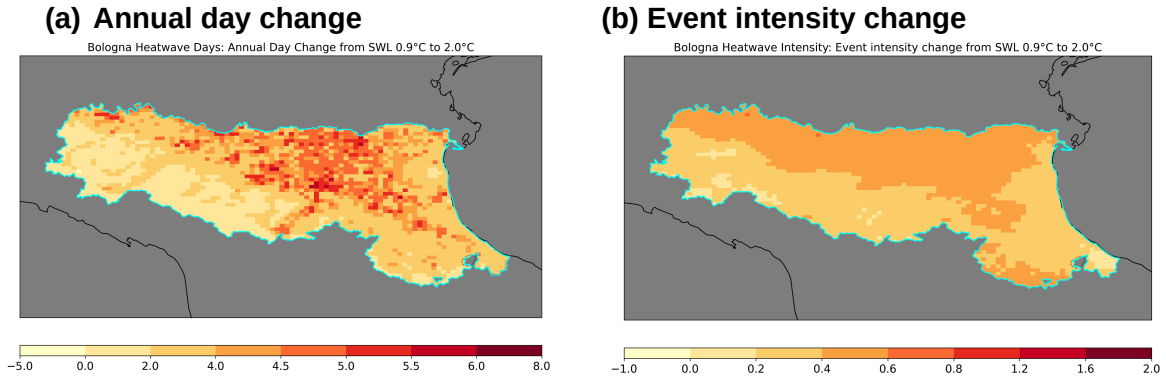


Figure 22. Spatial distribution of daytime temperature characteristic changes between RC and NMC based on Bologna heatwave events across the Emilia–Romagna region. (a) Annual Day Changes: Absolute change in the total number of days meeting heatwave criteria per year. (b) Event Intensity Changes: Difference in the composite mean temperature (°C) of heatwave events. Both panels represent the delta between the RC and NMC with positive values (red) indicating an increase in frequency and magnitude across the entire study domain.

6.2.2 Changes of heatwave events characteristics over tropical nights

To further investigate how nighttime temperatures change during these extreme events, we examined the daily minimum temperature (Tmin) associated with the Tmax-based urban heatwave events identified over the Bologna region and analyzed their projected changes under warmer climate conditions. Although the heatwave events are defined using daytime Tmax thresholds, the associated nighttime Tmin responses exhibit distinct spatial characteristics across Emilia–Romagna. Similar to the daytime analysis, the annual number of nighttime heatwave days increases substantially across the entire region, with the strongest increases occurring over the lowland and urbanized sectors of the Po Valley. The spatial distribution shown in Figure 23 reveals a clear topographic contrast between the lowland plains and mountainous regions, exhibiting a pattern broadly similar to the Tmax-based changes but with substantially stronger Tmin increases. The histogram analysis further indicates that more than one-third of the regional grid points experience increases of approximately 5 additional nighttime heatwave days between RC and NMC, while only a small fraction of the domain shows little or no change (Figure 23). These results demonstrate a robust and spatially consistent enhancement of nocturnal heatwave occurrence across Emilia–Romagna. Compared to the daytime Tmax distribution, the Tmin-related changes are also more spatially homogeneous and widespread, indicating that nocturnal warming affects a broader portion of the region.

The projected changes in nighttime heatwave intensity, represented by the composite mean Tmin during the Tmax-defined heatwave events, also exhibit a stronger and more spatially coherent warming signal than the corresponding daytime intensity changes (cf. Figure 21, 22). While daytime heatwave intensity increases were generally moderate, nighttime Tmin intensity increases approach or locally exceed 1 °C over large parts of the domain. The largest fraction of regional grid points, approximately 10–12% of the domain, experiences Tmin intensity increases around 0.7 - 0.9 °C, with most areas exhibiting warming between approximately 0.5 °C and 1.0 °C. Only a very limited fraction of the region shows weak or near-neutral intensity changes. These results suggest that additional warming not only increases the occurrence frequency of daytime heatwave events but also substantially enhances nocturnal heat retention during these events. Persistent high temperatures during both daytime and nighttime are particularly critical for human health, as reduced nighttime cooling limits physiological recovery from daytime heat exposure and can significantly increase cumulative thermal stress, heat-related illness, and mortality risks, especially in densely populated and urbanized environments.

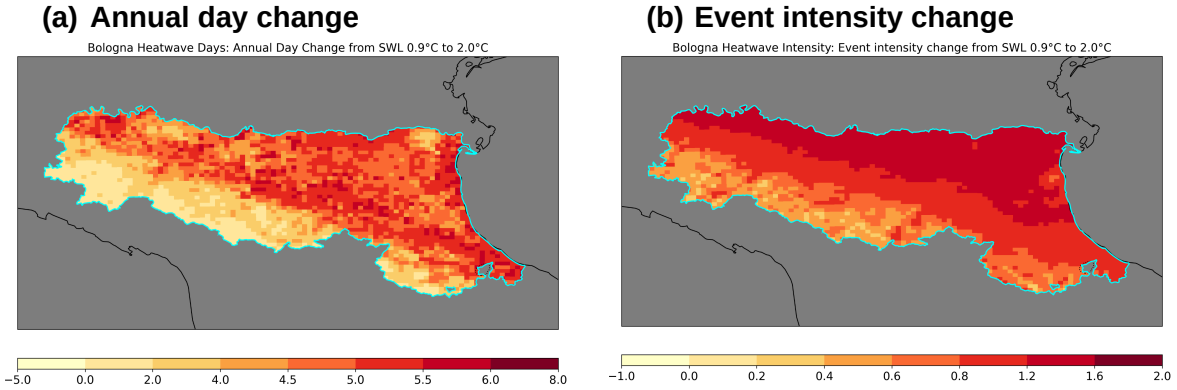


Figure 23. Spatial distribution of nighttime temperature characteristic changes between RC and NMC based on Bologna heatwave events across the Emilia–Romagna region. (a) Annual Day Changes: absolute change in the total number of nighttime heatwave days per year, defined using days with Tmin exceeding 20 °C. (b) Event Intensity Changes: Difference in the composite mean Tmin (°C) of nighttime heatwave events. Both panels represent the delta between the RC and NMC, with positive values (red) indicating increased nighttime heatwave frequency and enhanced nocturnal thermal intensity across most of the study domain.

6.3 Synthesis:

The analyses presented in this report demonstrate the potential of the event-based downscaling (EBD) framework to provide physically consistent climate information for high-impact weather events over the Emilia–Romagna region. By combining large-scale event detection from a large ensemble global climate simulation with convection-permitting regional climate modelling, the framework enables the generation of large samples of plausible extreme-event realizations under both present-day and future climate conditions. This approach bridges the gap between traditional climate projections and predictions and stakeholder-oriented information needs by focusing directly on weather events associated with societal impacts.

For Extreme Precipitation Events (EPEs), the EBD framework successfully reproduces the observed large-scale circulation characteristics associated with northern Italian heavy rainfall events, including the presence of upper-level troughs, enhanced moisture transport, and favorable synoptic conditions identified in previous studies of Mediterranean and Alpine precipitation extremes. The dynamically downscaled simulations produce substantially higher, more realistic, rainfall intensities than the driving global model, highlighting the added value of convection-permitting modelling for representing localized and convective precipitation processes. The analyses further indicate that moderate-to-strong extreme rainfall events become more frequent under warmer climate conditions, whereas the

response of the most extreme events is less robust and depends on the event-selection methodology and the limited number of available EBD samples.

For urban heatwave events, the EBD simulations indicate a clear intensification of both daytime and nighttime heat stress under warmer climate conditions. In particular, the duration and spatial extent of tropical nights increase substantially, indicating enhanced nocturnal heat stress across urban and lowland areas. These changes are consistent with the expected thermodynamic response to climate warming and highlight increasing heat-related risks for densely populated regions. Unlike precipitation, the projected heatwave response exhibits a much clearer and more robust climate-change signal, reflecting the dominant influence of thermodynamic warming. The EBD framework enables these changes to be resolved at convection-permitting resolution, providing detailed information on regional and urban-scale heat extremes that cannot be represented by global climate models. Such information is directly relevant for human health, urban planning, and climate adaptation, where local-scale temperature variations strongly influence heat exposure and associated risks.

The results also illustrate the strengths and limitations of the EBD approach. The framework efficiently samples rare events by targeting physically relevant weather situations rather than relying on continuous transient simulations, making it particularly suitable for stakeholder applications that require detailed information on high-impact events. At the same time, uncertainty increases rapidly for very rare events because the estimation relies on a limited number of event samples. The widening confidence intervals at long return periods demonstrate that the statistical robustness of the most extreme tail of the distribution remains limited. Furthermore, the present prototype is based on a single driving global climate model and a single warming storyline. Consequently, the uncertainty estimates presented here primarily reflect sampling variability and the statistical fitting procedure, while uncertainties associated with climate-model structure, event-detection methodology, regional-model configuration, and future forcing pathways are not represented.

Overall, the EBD framework provides a scientifically credible and computationally efficient approach for producing event-focused climate information relevant to adaptation planning. The results suggest increasing heat-related risks and changes in extreme precipitation characteristics over Emilia–Romagna under mid-century climate conditions, while also highlighting the importance of considering uncertainty when interpreting projections of the most extreme and rare events. Future developments should expand the framework to multiple climate models, warming scenarios, and larger event samples in order to provide a more comprehensive quantification of uncertainty and improve confidence in estimates of high-return-period extremes.

7. Future applicability of scalable prototype

For the first time, this deliverable shows that a convection-permitting regional climate model can be applied within an Event-Based Downscaling (EBD) framework to investigate regional

climate-change impacts on extreme weather events that are only partially represented in coarse-resolution global climate models. The prototype implementation developed for the Emilia–Romagna region combines standardized procedures for event detection, model spin-up, and automated simulation workflows, enabling the downscaling of large numbers of multi-day extreme events under different climate conditions. The resulting catalogue provides a practical basis for assessing changes in regional climate extremes and serves as a proof-of-concept for broader application of the EBD framework.

The question of scalability has three dimensions: **(i) Transferability to different regions, (ii) Applicability to different types of global climate simulations**, and **(iii) Applicability for different use cases and user communities**.

Transferability across regions: The EBD framework has already been transferred beyond the Emilia–Romagna case study and applied in related projects, including Swedish national projects, UrbExtDT and Green4Extremes, for urban regions in Gothenburg and Malmö, Sweden. The application in new regions requires an evaluation under past and recent climate conditions to benchmark simulation quality and suitable definitions of extreme events for the respective region. The remaining setup of automatic spinup and simulations is unchanged. Due to the sensitivity of results to the choice of detection method, this sensitivity will also need to be documented for new regions. With the system developed under ASPECT WP3, the effort for application of EBD for new regions is modest (a week for an experienced scientific engineer).

Applicability to different global climate simulations: The current prototype of EBD has been developed with the example of a large ensemble of a global model projection (EC-Earth3, 50 members) as forcing. In principle, the method is transferable to any kind of global model forcing that provides necessary lateral boundary conditions for the regional climate model that is used for EBD.

A sizable number of CMIP6 and CMIP6 style ESMs export necessary data under an agreement with CORDEX under the umbrella of a CORDEXMIP under CMIP. The necessary forcing data for EBD is regularly provided to CORDEX 10 km and 25 km downscaling for various regional domains. Those CMIP6 and CMIP7 ESMs could be interpreted for extreme events (which they do not fully represent) by application of the EBD method

Many current standard set ups of initialized global prediction models usually do not export the necessary level data for regional downscaling. This issue is a matter of coordination. For limited time periods, ensemble size and geographical region, global climate prediction models could be able to export necessary data.

A workaround for the issue in the previous bullet point (limited data export from standard initialized global prediction models) is a time merging method which combines multi-annual prediction ensembles with uninitialized ESM projections: Corresponding approaches are performed in task 3.3 which leads to selection of projections which are compatible with predictions. Those sub-sampled CMIP projections (which partly export lateral boundary

conditions for EBD) could potentially be used for downscaling. “Shadowing” or “Constraining” methods (see forthcoming deliverable D3.4) select ensemble members from long-term simulations that closely follow higher-quality short-term trajectories, such as observations or near-term forecasts. The underlying assumption is that these selected trajectories will continue to evolve close to the true climate state in the unknown future. In this context, Barcelona Supercomputing Center have explored and compared several approaches to constrain variability in large multi-model ensembles of climate projections. These constraints aim to extend the influence of initialisation information beyond the typical 10-year limit of decadal predictions, thereby enabling seamless decadal-to-multi-decadal climate information. A recent study by Donat et al., 2024 demonstrates the use of observational- and decadal-prediction-based constraints to a large multi-model ensemble.

AI emulators of the dynamic downscaling model as under development in parallel projects could potentially be used to downscale events without the need of exhaustive complete lateral boundary conditions.

Applicability for different use cases and user communities: Scalability across different use cases and user communities has been investigated within ASPECT WP5 from a social-science perspective. The WP5 analyses highlight that upscaling climate services, including methodologies such as EBD, is not merely a matter of applying downscaling methods to larger domains or a greater number of users. Instead, successful upscaling requires transferring co-produced climate information into broader operational and decision-making contexts. Usability, accessibility, and integration into sector-specific workflows are identified as being as important as the scientific quality of the climate information itself, while institutional capacity, governance structures, and trust-building are recognized as key enabling factors for wider adoption.

These findings are consistent with the experience gained during the development of the Emilia–Romagna prototype. Throughout the project, close collaboration with ARPAE ensured that the selection of climate hazards, event definitions, diagnostics, and climate information products was guided by regional adaptation needs. This iterative co-design process resulted in several case-specific methodological developments, including tailored detection approaches for EPEs and heatwaves, as well as the development of impact-relevant indicators designed to support regional risk assessment and climate-service applications. The experience demonstrates that the value of EBD lies not only in producing high-resolution climate information, but also in its flexibility to incorporate stakeholder priorities and adapt the methodology to specific decision-making contexts.

Based on these experiences, future developments of the EBD framework should consider a broader range of use cases and application contexts beyond the specific hazards and stakeholder needs addressed within ASPECT. The Swedish UrbExtDT project provides an example of how the flexibility of EBD can facilitate transfer to new application domains. While ASPECT focused on the co-development of event-based climate information for regional climate hazards in Emilia–Romagna, UrbExtDT extends similar EBD concepts to urban adaptation planning in Sweden and South Africa. In this context, the methodology is

integrated with digital twins, machine-learning tools, visualization platforms, and scenario-analysis frameworks, addressing challenges that differ substantially from those considered in ASPECT. These experiences suggest that the successful scaling of EBD is not achieved by simply replicating a technical workflow across different regions and sectors. Rather, scalability relies on maintaining a common scientific framework while allowing hazard definitions, climate indicators, workflows, and service products to be adapted to local user needs and operational contexts. Future developments should therefore place equal emphasis on methodological robustness, stakeholder co-production, and integration into decision-support systems to maximize the societal relevance and usability of EBD-based climate information.

References

Agenzia Regionale per la Prevenzione, l'Energia e l'Ambiente dell'Emilia-Romagna. (2023). *ERG5 - Interpolazione su griglia di dati meteo* [Data set]. Retrieved June 15, 2025, from https://dati.arpae.it/dataset/erg5-interpolazione-su-griglia-di-dati-meteo

Antolini, G., Auteri, L., Pavan, V., Tomei, F., Tomozeiu, R. and Marletto, V. (2016). A daily high-resolution gridded climatic data set for Emilia-Romagna, Italy, during 1961–2010. *Int. J. Climatol.*, 36: 1970-1986. doi:10.1002/joc.4473.

Belušić, D., de Vries, H., Dobler, A., Landgren, O., Lind, P., Lindstedt, D., Pedersen, R. A., Sánchez-Perrino, J. C., Toivonen, E., van Ulft, B., Wang, F., Andrae, U., Batrak, Y., Kjellström, E., Lenderink, G., Nikulin, G., Pietikäinen, J.-P., Rodríguez-Camino, E., Samuelsson, P., van Meijgaard, E., & Wu, M. (2020). HCLIM38: A flexible regional climate model applicable for different climate zones from coarse to convection-permitting scales. *Geoscientific Model Development*, 13(3), 1311–1333. https://doi.org/10.5194/gmd-13-1311-2020

Bloin-Wibe, L., Noyelle, R., Humphrey, V., Beyerle, U., Knutti, R., and Fischer, E. (2025). Estimating return periods for extreme events in climate models through Ensemble Boosting. Weather and Climate Dynamics, 6: 1147–1177. doi:10.5194/wcd-6-1147-2025.

Brajkovic, J., Archambeau, P., Ghilain, N., and Doutreloup, S.: Past and future evolution of cut-off-low-associated extreme precipitation in Europe, EGUsphere [preprint], https://doi.org/10.5194/egusphere-2026-2315, 2026.

Cavalleri, F., Lussana, C., Viterbo, F., Brunetti, M., Bonanno, R., Manara, V., Lacavalla, M., and Maugeri, M. (2026). Hourly precipitation patterns and extremization over Italy using convection-permitting reanalysis data. Natural Hazards and Earth System Sciences, 26: 279–297. doi:10.5194/nhess-26-279-2026.

Coles, S. (2001). An Introduction to Statistical Modeling of Extreme Values. London: Springer-Verlag London. doi:10.1007/978-1-4471-3675-0.

Cornes, R. C., van der Schrier, G., van den Besselaar, E. J. M., & Jones, P. D. (2018). An ensemble version of the E-OBS temperature and precipitation data sets. Journal of Geophysical Research: Atmospheres, 123, 9391–9409. https://doi.org/10.1029/2017JD028200

Coppola, E., Nogherotto, R., Ciarlò, J. M., Giorgi, F., van Meijgaard, E., Kadygrov, N., et al. (2021). Assessment of the European Climate Projections as Simulated by the Large EURO-CORDEX Regional and Global Climate Model Ensemble. Journal of Geophysical Research: Atmospheres, 126, e2019JD032356. https://doi.org/10.1029/2019JD032356

Coppola, E., Pons, F. M. E., Alberti, T., Portal, A., & Faranda, D. (2024). *October 2024 Italy multiple floods mostly strengthened by human-driven climate change*. ClimaMeter, Institut Pierre Simon Laplace, CNRS. https://doi.org/10.5281/zenodo.1405462

Danielson, J. J., & Gesch, D. B. (2011). *Global multi-resolution terrain elevation data 2010 (GMTED2010)* (Open-File Report 2011-1073). U.S. Geological Survey. https://doi.org/10.3133/ofr20111073

Davolio, S., Volonté, A., Manzato, A., Pucillo, A., Cicogna, A. and Ferrario, M.E. (2016), Mechanisms producing different precipitation patterns over north-eastern Italy: insights from HyMeX-SOP1 and previous events. Q.J.R. Meteorol. Soc., 142: 188-205. https://doi.org/10.1002/qj.2731.

Dorigo, W. A., Wagner, W., Albergel, C., Albrecht, F., Balsamo, G., Brocca, L., Chung, D., Ertl, M., Forkel, M., Gruber, A., Haas, E., Hamer, P. D., Hirschi, M., Ikonen, J., de Jeu, R., Kidd, R., Lahoz, W. A., Liu, Y. Y., Miralles, D., Lecomte, P., et al. (2017). ESA CCI Soil Moisture for improved Earth system understanding: State-of-the-art and future directions. Remote Sensing of Environment, 203, 185–215. doi:10.1016/j.rse.2017.07.001.

Donat, M. G., et al. (2024). *Environmental Research: Climate*, *3*(3), Article 035013. https://doi.org/10.1088/2752-5295/ad5463

Efron, B., & Tibshirani, R.J. (1994). An Introduction to the Bootstrap (1st ed.). Chapman and Hall/CRC. doi: 10.1201/9780429246593.

Grazzini, F., Craig, G. C., Keil, C., Antolini, G., and Pavan, V. (2020). *Extreme precipitation events over northern Italy. Part I: A systematic classification with machine-learning techniques*. *Quarterly Journal of the Royal Meteorological Society*, 146(726): 69–85. doi:10.1002/qj.3635.

Grazzini, F., Fragkoulidis, G., Teubler, F., Wirth, V., and Craig, G. C. (2021). *Extreme precipitation events over northern Italy. Part II: Dynamical precursors*. Quarterly Journal of the Royal Meteorological Society, 147(735): 1237–1257. doi:10.1002/qj.3969.

Hersbach, H., Bell, B., Berrisford, P., Hirahara, S., Horányi, A., Muñoz-Sabater, J., Nicolas, J., Peubey, C., Radu, R., Schepers, D., Simmons, A., Soci, C., Abdalla, S., Abellan, X., Balsamo, G., et al. (2020). The ERA5 global reanalysis. *Quarterly Journal of the Royal Meteorological Society*, 146(730): 1999–2049. doi:10.1002/qj.3803.

Kelso, N. V., & Patterson, T. (2010). Natural Earth (Version [Insert Version, e.g., 5.1.0]) [Map dataset]. North American Cartographic Information Society. https://www.naturalearthdata.com

Lindstedt, D., Lind, P., Kjellström, E. & Jones, C. (2015) A newregional climate model operating at the meso-gamma scale:performance over Europe. *Tellus A: Dynamic Meteorology and Oceanography*, 67(1), 24,138.

Massacand, A. C., Wernli, H., & Davies, H. C. (1998). Heavy precipitation on the Alpine southside: An upper-level precursor. *Geophysical Research Letters, 25*(9), 1435–1438. https://doi.org/10.1029/98GL50869

Miglietta, M. M. and Davolio, S.: Dynamical forcings in heavy precipitation events over Italy: lessons from the HyMeX SOP1 campaign, Hydrol. Earth Syst. Sci., 26, 627–646, https://doi.org/10.5194/hess-26-627-2022, 2022.

Mishra, A.N., Maraun, D., Schiemann, R. *et al.* (2025). Long-lasting intense cut-off lows to become more frequent in the Northern Hemisphere. *Commun Earth Environ* **6**, 115. https://doi.org/10.1038/s43247-025-02078-7

Pavan, V., Tomozeiu, R., Cacciamani, C., and Di Lorenzo, M. (2008). Daily precipitation observations over Emilia-Romagna: Mean values and extremes. International Journal of Climatology, 28(15): 2065–2079. doi:10.1002/joc.1694.

Pfahl, S. (2014). Characterising the relationship between weather extremes in Europe and synoptic circulation features, Nat. Hazards Earth Syst. Sci. 14, 1461–1475, doi.org:10.5194/nhess-14-1461-2014.

Prein, A. F., Langhans, W., Fosser, G., Ferrone, A., Ban, N., Goergen, K., et al. (2015). A review on regional convection-permitting climate modeling: Demonstrations, prospects, and challenges. *Reviews of Geophysics*, 53(2): 323–361. doi:10.1002/2014RG000475.

Raveh-Rubin, S. and Wernli, H. (2015), Large-scale wind and precipitation extremes in the Mediterranean: a climatological analysis for 1979–2012. Q.J.R. Meteorol. Soc., 141: 2404-2417. doi.org:10.1002/qj.2531.

Sabatani, D., Pavan, V., Grazzini, F., and Antolini, G. (2024). Long-term trend and variability in surface temperatures over Emilia-Romagna from 1962 to 2022. Theoretical and Applied Climatology, 155(11–12): 6297–6305. doi:10.1007/s00704-024-04994-8.

Seity, Y., Brousseau, P., Malardel, S., Hello, G., Bénard, P., Bouttier, F., Lac, C., and Masson, V. (2011). The AROME-France convective-scale operational model. *Monthly Weather Review*, 139(3): 976–991. doi:10.1175/2010MWR3425.1.

Sobolowski, S., and Coauthors (2025). GCM Selection and Ensemble Design: Best Practices and Recommendations from the EURO-CORDEX Community. *Bull. Amer. Meteor. Soc.*, **106**, E1834–E1850, doi.org/10.1175/BAMS-D-23-0189.1.

Tomozeiu, R., Cacciamani, C., Amici, M., and Pavan, V. (2006). Observed temperature changes in Emilia-Romagna: Mean values and extremes. Climate Research, 31(2–3): 217–225. doi:10.3354/cr031217.

Valente, M., Del Prete, C., Facci, G., Martino, A., Grilli, G. R., Bravi, F., Reno, C., & Ragazzoni, L. (2025). The 2023 floods in the Emilia-Romagna Region, Italy: A retrospective qualitative investigation into response strategies and criticalities. International Journal of Disaster Risk Reduction, 116, Article 105089. doi: 10.1016/j.ijdrr.2024.105089

Villani, G., Tomei, F., Pavan, V., Pirola, A., Spisni, A., & Marletto, V. (2021). The iCOLT climate service: Seasonal predictions of irrigation for Emilia-Romagna, Italy. Meteorological Applications, 28(4), e2007. https://doi.org/10.1002/met.2007

Wyser, K., Koenigk, T., Fladrich, U., Fuentes-Franco, R., Karami, M. P., and Kruschke, T. (2021). The SMHI Large Ensemble (SMHI-LENS) with EC-Earth3.3.1. *Geoscientific Model Development*, 14(8): 4781–4796. doi:10.5194/gmd-14-4781-2021.

Supplementary Material

Table S1. Abbreviation table

Abbreviation Table	
Abbreviation	**Full name**
AI	Artificial Intelligence
ARPAE	Agenzia Regionale per la Prevenzione, l'Ambiente e l'Energia dell'Emilia-Romagna
ArCIS	Climatological Archive for Central–Northern Italy
CAPE	Convective Available Potential Energy
CDF	Cumulative Distribution Function
CMIP6	Coupled Model Intercomparison Project Phase 6
CMOR	Climate Model Output Rewriter
CP	Convection-Permitting
CPRCM	Convection-Permitting Regional Climate Model
DEM	Digital Elevation Model

EBD	Event-Based Downscaling
EC-Earth3	European Community Earth-System Model version 3
ECMWF	European Centre for Medium-Range Weather Forecasts
ECOCLIMAP	ECOCLIMAP land cover database
E-OBS	European Observation Dataset
ERA5	ECMWF Reanalysis version 5
ERA-Interim	ECMWF Interim Reanalysis
ER	Emilia–Romagna
ERG5	Emilia–Romagna 5 km Gridded Dataset
ESA	European Space Agency
ESA CCI	ESA Climate Change Initiative
EPE	Extreme Precipitation Event
EU	European Union

EURO-CORDEX	European Coordinated Regional Climate Downscaling Experiment
EVT	Extreme Value Theory
GCM	Global Climate Model
GEV	Generalized Extreme Value
HCLIM	HARMONIE Climate Model
LENS	Large Ensemble Simulation
NMC	Near Mid-century Climate
PDF	Probability Density Function
RC	Recent Climate
RCM	Regional Climate Model
SCI	Seamless Climate Information
SMHI	Swedish Meteorological and Hydrological Institute

SMHI-LENS	SMHI Large Ensemble
SSP3-7.0	Shared Socioeconomic Pathway 3–7.0
SURFEX	Surface Externalisée
Tmax	Daily Maximum Temperature
Tmin	Daily Minimum Temperature
WP	Work Package

Table S2. Atmospheric and land fields

Atmospheric and land fields				
Variable	**Short name**	**Units**	**Frequency**	**Description**
Near surface air temperature	tas	K	1hr	Instantaneous
Daily maximum near surface air temperature	tasmax	K	day	Daily max
Daily minimum near surface air temperature	tasmin	K	day	Daily min
Near surface specific humidity in air	huss	1	1hr	Instantaneous
Near surface relative humidity in air	hurs	%	1hr	Instantaneous
Near surface zonal wind	uas	m s-1	1hr	Instantaneous
Near surface meridional wind	vas	m s-1	1hr	Instantaneous
Near surface wind speed	sfcWind	m s-1	1hr	Instantaneous
Sea level pressure	slp	Pa	1hr	Instantaneous
Surface pressure	sp	Pa	1hr	Instantaneous
Total precipitation	pr	kg m-2 s-1	1hr / day	Accumulated
Snowfall precipitation	prsn	kg m-2 s-1	1hr / day	Accumulated

Total cloud cover	clt	%	1hr	Accumulated
Evaporation flux	evpsbl	kg m-2 s-1	1hr	Accumulated
Downward shortwave at surface	rsds	W m-2	1hr	Accumulated
Upward shortwave at surface	rsus	W m-2	1hr	Accumulated
Downward longwave at surface	rlds	W m-2	1hr	Accumulated
Upward longwave at surface	rlus	W m-2	1hr	Accumulated
Latent heat flux at surface	hfls	W m-2	1hr	Accumulated
Sensible heat flux at surface	hfss	W m-2	1hr	Accumulated
Skin temperature	ts	K	1hr	Instantaneous
Sea surface temperature	tos	K	1hr	Instantaneous
Surface runoff	mrros	kg m-2 s-1	6hr	Accumulated
Subsurface runoff	mrrod	kg m-2 s-1	6hr	Accumulated
Soil temperature (14 levels)	tsl	K	6hr	Instantaneous
Soil moisture (14 levels)	mrsol	kg m-2	6hr	Instantaneous

In addition to the atmospheric and land variables, a set of physiographic fields is also included:

Table S3. Physiographic fields

Physiographic fields			
Variable	**Short name**	**Units**	**Description**
Field capacity of soil	mrsofc	kg m-2	Integrated over the upper 12m of soil column.
Surface altitude	orog	m	
Fraction of grid cover by land	sftlf	%	
Fraction of grid cover by lakes	sftlaf	%	
Fraction of grid covered by urban areas	sfturf	%	
Fraction of grid covered by covers of ECOCLIMAP-SG	sftlulc	%	33 different land use covers.
Fraction of grid where SMR is applied*	smrmask	%	

**only available in heatwave simulations.*